1. Using fragment-based drug design to inhibit RAGE-ligand interactions

Natalia Kozlyuk

The receptor for advanced glycation end products (RAGE) is a multi-ligand pattern recognition cell surface receptor, which upon activation stimulates intracellular inflammatory signaling with implications in diabetes, arthritis, Alzheimer's and other diseases. The overall objective of this project is to develop inhibitors of RAGE-ligand interactions to discern the mechanism of RAGE activation and downstream signaling, as well as to lay the foundation to evaluate the therapeutic potential of inhibiting RAGE to suppress the disease-associated chronic inflammatory processes. To this end, we have first focused on targeting RAGE and screened a small, curated fragment library using the 'structure activity relationship (SAR) by NMR' approach. For hit fragments, I determined the orientation and the exact location of the hit fragments bound to RAGE using X-ray crystallography. Fragment molecules were discovered that bound to different sites on RAGE, 4.2 Å apart. In collaboration with Alex Waterson here at Vanderbilt, information from the crystal structures along with the concepts of medicinal chemistry were then utilized to chemically elaborate fragments and increase their affinities for RAGE as well as bring them closer together by 0.5 Å. Working iteratively with structures, design and the Vanderbilt Chemical Synthesis Core, pairs of fragments are being linked together to generate multivalent high affinity compounds.

2. Identification of ZNF280C as a novel fork stabilization protein

Wenpeng Liu

ZNF280C is a 81Kda Zinc finger domain containing protein, located in chromosome X, Broad expression in testis (RPKM 6.8), endometrium (RPKM 1.7) and 21 other tissues. It has other names are SUHW3 (suppressor of hairy wing homolog 3) and ZNF633(zinc finger protein 633). We screen the protein enriched on stalled fork by IPOND (Isolation of Proteins on Nascent DNA) method, results shows ZNF280C enriched on stalled fork in response to HU treatment. We find that in U2OS cells, depletion of ZNF280C leads to significant increase of gH2AX, as well as RAD51 and phosphorylated RPA2. Combine knockdown of SLX4 nuclease can reduce or eliminate gH2AX in absence of ZNF280C. We use fiber assay to determine if ZNF280C knockdown affect the stalled fork restart and fork degradation. Results shows that, in absence of ZNF280C, stalled replication fork is over resected than control, the restart efficiency also impaired by ZNF280C knockdown. We concluded that ZNF280C is a novel fork stabilization protein that can protect nascent DNA from degradation in response to replication stress. Its functions need to further study.

3. Implementation of 193 nm ultraviolet photodissociation on a Fourier transform ion cyclotron resonance mass spectrometer for lipid and peptide identification

Boone M. Prentice, Daniel J. Ryan, Eric C. Spivey, Jeffrey M. Spraggins, Richard M. Caprioli

Matrix-assisted laser desorption/ionization imaging mass spectrometry (MALDI IMS) is a powerful technology that provides for the generation of molecular maps of lipid and protein distributions in organ tissue sections. A key step in any IMS workflow is the unambiguous chemical identification of the specific lipid and/or protein ions of interest. This identification is often performed via a combination of an accurate mass measurement, which is used to determine the elemental composition of the ion, and tandem mass spectrometry (MS/MS), which involves fragmenting the ion inside the mass spectrometer to determine chemical structure. Though several current MS/MS methods exist, these workflows often provide incomplete sequence information for lipids and proteins generated via MALDI.

Herein, we have implemented 193 nm ultraviolet photodissociation (UVPD) on a Fourier transform ion cyclotron resonance mass spectrometer (FT-ICR MS) to enable improved sequencing of lipids and proteins. The UVPD setup consists of an optical periscope to level and align the laser beam through a quartz window installed on the instrument vacuum manifold. Triggering and timing of the UVPD pulse sequence is controlled using a transistor-transistor logic (TTL) signal from the mass spectrometer that is then shaped using a pulse generator before being fed into the UVPD external trigger input. This setup allows for in-cell tandem mass spectrometry to be performed on mass-selected lipid and protein ions.

UVPD as a chemical identification strategy uniquely allows for the localization of double bonds in the fatty acyl chains of phospholipids and also induces fragmentation in a relatively unbiased manner across peptide backbones, allowing for extensive sequence coverage and accurate analyte identification. We have demonstrated the utility of this methodology using model lipid (phosphatidylcholine, phosphatidylinositol) and peptide (substance P, insulin chain B) compounds. Briefly, these analytes are stored in the ICR cell and irradiated using 193 nm UVPD in order to induce fragmentation. Irradiation is performed using pulse energies of 3-10 mJ for 3-50 pulses, depending on the analyte of interest. The extensive sequence coverage afforded by UVPD will enable better identification of lipid and protein species detected during imaging mass spectrometry experiments.

4. Synthesis of N7-Methyl Deoxyguanosine Adduct for the Evaluation of Miscoding Events by DNA Polymerases

Olive Njuma and F. Peter Guengerich

DNA is prone to damage from several endogenous and exogenous sources such as reactive oxygen species, UV light, chemical contaminants, and societal habits. Specifically, the N and O positions of DNA bases are readily alkylated by several known alkylating agents, leading to different types of DNA damages. If not repaired immediately, such damage can lead to miscoding events and mutations, which have detrimental consequences to health causing cancer, teratogenesis, cardiovascular problems, and aging. N^7-Alkyl deoxyguanosine (dGuo) is one type of DNA damage that has been ignored in favor of other alkylated bases. This DNA

adduct is known to have unstable glycosidic bonds and hence tend to depurinate, although its rate of depurination is relatively slow. Initial evidence based on older techniques suggested that this adduct is not miscoding but we hypothesize that there exists a potential for miscoding. We are employing a 2'-fluoro isostere approach to produce stable analogs of this oligonucleotide. We will use modern methods such as LC-MS/MS, pre-steady-state kinetics, and X-ray crystallography to evaluate the incidence of miscoding events by different bacterial and human DNA polymerases. Evaluating the chemistry and biology of these lesions is critical for assessing their risks.

5. Synthesis and Bypass Studies of AGT-DNA Cross-links

Pratibha P. Ghodke and F. P. Guengerich

O^6-Alkylguanine DNA-alkyltransferase (AGT) protein is known to form DNA crosslinks *in vivo* with 1,2-dibromoethane (a potent carcinogen).[1] The hypothesis to be addressed is that AGT-DNA crosslinks formed are processed by cellular proteases[2] to yield peptides that are small enough to be bypassed by low fidelity polymerases (TLS polymerases). To test this hypothesis, an efficient methodology is needed for the synthesis of DNA-protein cross-links substrates. Toward this end, we developed a synthesis of AGT-DNA cross-link at the *N*^{2} position of guanine as well as *N*^{6} position of adenine (**Figure 1**) employing click chemistry. The purification of these cross-links using different techniques are in progress. After having pure crosslinks in hand, we will test the hypothesis, which involves characterization of the crosslinked peptides and how they interact with the DNA polymerases during bypass studies. These studies can help to understand how a DNA pol can bypass a very large entity as well as the base pair mutations generated by AGT crosslinks.

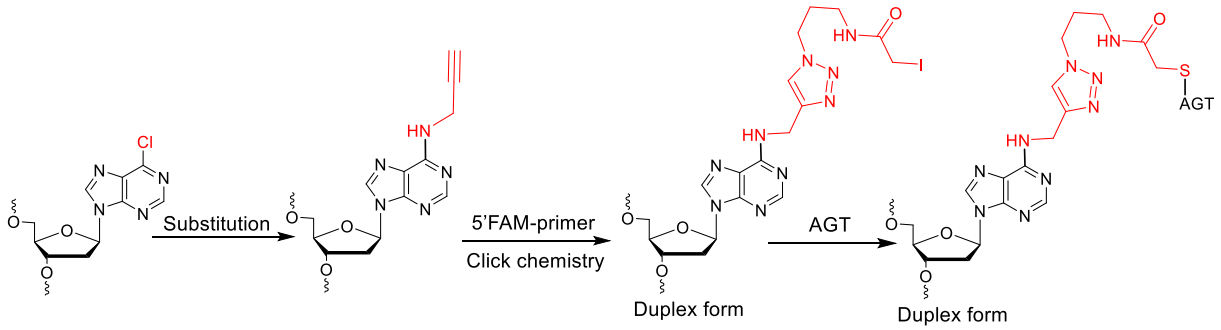

Figure 1: Synthetic strategy for the DNA-protein cross links at *N*^{6}-position of adenine

References:

1. Chowdhury G., Cho S-H, Pegg A. E., Guengerich F. P. *Angew. Chem. Int. Ed.* **2013**, 52, 12879-12882.
2. Stingele J., Schwarz M. S., Bloemeke N., Wolf P. G., Jentsch S. A., *Cell* **2014**, 158, 327-338

6. Nuclear Localized Raf1 Isoform Alters DNA-dependent Protein Kinase Activity and the DNA Damage Response

Benjamin Nixon

Raf1/c-Raf is a well characterized serine/threonine-protein kinase that links Ras family members with the MAPK/ERK signaling cascade. We have identified a novel splice isoform of human Raf1

that causes protein truncation and loss of the C-terminal kinase domain (Raf1-tr). We found that Raf1-tr has increased nuclear localization compared to full length Raf1 and this was secondary to reduced binding of Raf1-tr to the cytoplasmic chaperone FKBP5. We demonstrate that Raf1-tr has increased binding to DNA-dependent Protein Kinase (DNA-PK), which inhibits DNA-PK function, and causes amplification of bleomycin induced DNA damage. Finally, we found that the human colorectal cancer cell line, HCT-116, displayed reduced expression of Raf1-tr and reintroduction of Raf1-tr sensitized the cells to bleomycin-induced apoptosis. Collectively, these results demonstrate a novel Raf1 isoform in humans that has a unique non-canonical role in regulating the double stranded DNA-damage response pathway through modulation of DNA-PK function.

7. Fatty Acid B-oxidation and Synthesis in BRAF-mutated Melanomas Is Uncoupled From Proliferation

Keisha Hardeman, Bishal Paudel, Chengwei Peng, Vito Quaranta, and Joshua Fessel

The metabolic landscape of cancer resistance remains largely unknown, particularly in the context of oncogenic lesions such as mutant BRAF kinase. Our previous work showed that glucose is a key nutrient influencing response to pharmacologic BRAF inhibition in BRAF-mutated melanomas. Despite heterogeneous metabolic programs, these melanomas are addicted to oxidative phosphorylation through mitochondria, and we leveraged that metabolic dependency to a fault by forcing glycolysis at the expense of mitochondrial respiration. This approach increased sensitivity to BRAF inhibition and opened questions of how metabolite utilization and signal transduction intersects. Using substrate-inhibitor combinations targeting fatty acids, glutamine, and pyruvate, we found that these melanomas have an absolute requirement of fatty acid oxidation (FAO) for ATP-linked oxygen consumption. Interestingly, however, FAO is not necessary for these cells to proliferate: inhibition of the rate-limiting FAO enzyme CPT1 has minimal effect on proliferation rates. Additionally, co-targeting mutant-BRAF and MEK did not allow FAO to modulate proliferative outcomes, so we investigated whether the ATP production system is coupled to proliferation. Inhibition of ATP synthase with oligomycin universally affected all melanoma cells tested, and obliteration of the mitochondrial genome via ethidium bromide previously showed continued proliferation at a lower rate. Considering the cellular requirements of fatty acids for membrane building and physiology, we inhibited fatty acid synthesis (FAS) and observed robust decreases in proliferation. Conceptually, our working model suggests a dichotomized view of fatty acids broken down and oxidized for ATP (normal, oxidative direction) and fatty acids synthesized through reductive carboxylation (opposite direction).

8. Ion Mobility in support of Untargeted Metabolomics

Charles M. Nichols, James N. Dodds, Jody C. May, Jaqueline Picache, Bailey S. Rose, Stacy D. Sherrod, John A. McLean

Ion mobility (IM) usage is on the rise in metabolomics laboratories around the world. When the parameters are carefully characterized, IM measurements can be reported as collision cross section (CCS) values. CCS is a structural descriptor orthogonal to RT, m/z, and fragmentation. To best utilize IM technologies, CCS libraries must be generated to support molecular identification in untargeted metabolomics IM workflows. Traditional workflows for measuring absolute CCS are time consuming, and therefore we have developed novel, fully-automated

methods to measure CCS with commercial hardware and software. In addition to reporting these methods, we will discuss strategies to overcome the analytical challenges when measuring standards to report accurate, reliable CCS values. One aspect of this presentation will discuss a recent absolute CCS library we generated from the Mass Spectrometry Metabolite Library of Standards (MSMLS, Iroa Technologies). The MSMLS is a suite of over 620 chemical standards from several classes of biomolecules. In addition to the MSMLS, we have generated extensive database libraries of lipids from standards and extracts. One aspect of this presentation will discuss conformational trends of biological classes, and how these trends can be used to reject false positive identifications in untargeted experiments. This work will also present an application of CCS libraries to real data, i.e. the treatment of HL60 (peripheral blood, leukemia) cells with methotrexate (chemotherapeutic), to illustrate the utility of IM in untargeted experiments.

9. Codon usage in the Saccharomycotina - How the silent codon position can be used as window into gene expression and ecological adaptation

Abigail LaBella

Cracking the genetic code revealed that 18 of the 20 amino acids are encoded by degenerate codons. For example, TAT and TAC both code for the amino acid tyrosine but are not always used equally. Variation in codon usage occurs within single genes, across entire genomes and between different species. Differences in codon usage were once attributed solely to GC mutational bias. Recent evidence, however, suggests that codon usage plays a role in translation elongation, translation efficiency and mRNA stability. Selection on these processes is stronger in highly expressed genes resulting in a set of optimal codons that are decoded accurately and efficiently by abundant tRNAs. As a result, a gene's level of codon bias is strongly and significantly associated with its expression level. Here we take advantage of the vast genomic and ecological diversity of the yeasts subphylum Saccharomycotina to examine variation in codon usage and use this variation as a proxy for gene expression associated with ecological niche. Codon usage varies extensively across the Saccharomycotina, including in the only two known lineages with complete codon reassignment in a non-stop codon. Furthermore, by using codon bias as a proxy for gene expression we identify genes and pathways significantly associated with specific ecological niches. This work suggests that we can use genomic data to infer important ecological pathways in species where transcriptomics is not possible, such as in many of the microbes in the human microbiome.

10. The Center for Innovative Technology: A Collaborative Research Core for Metabolomics

Alexandra Rutledge

The Center for Innovative Technology supports investigators in untargeted metabolomic data acquisition and provides a number of routine and advanced services depending on individual research goals. The complex array of metabolites within a fluid, cell, or tissue can be measured and steady state or temporal changes can be determined for context-dependent global metabolomics analyses. Metabolite annotations are assigned based on high mass accuracy measurements, isotope distributions, tandem MS/MS spectra, and comparisons with

commercial spectral libraries. Results can reveal unique biochemical fingerprints of cellular processes specific to a sample group. These types of datasets can be exploited as a discovery-based approach for generating novel hypotheses or used for a better understanding of physiological processes mediated by genetic or environmental perturbations. Representative data is presented for alterations of epithelial cell metabolism in response to cigarette smoking condensate, a preliminary effort to reveal key molecular species involved in COPD pathogenesis.

11. The implications of human genetic diversity for structural biology

Gregory Sliwoski, Neel Patel, R. Michael Sivley, Jens Meiler, William S. Bush, John A. Capra

There is no single “wild-type” allele of most human proteins; multiple common sequence haplotypes are segregating for thousands of human proteins. However, studies that analyze the 3D structure of these proteins typically use a single “canonical” amino acid sequence. In this project, we quantify the diversity of protein sequences within and between human populations, and then evaluate the coverage of observed protein sequences by experimentally characterized 3D structures. We find that available protein structures often do not represent common sequences of the protein modeled, and African-ancestry sequences are less likely to be represented by available protein structures. Using structure, context, and annotation, we identify thousands of unmodeled variants with the potential to influence fold or function. In particular, we find 134 variants across 113 proteins that alter disulfide bonds, 1463 variants across 805 proteins in close proximity to a ligand, 322 variants across 148 proteins near complexed DNA, and 6144 variants across 1836 proteins that lie within a protein-protein interface. Further, we computationally modeled a subset of these variants’ effects on protein stability and interactions, and found that 156/556 (26%) are predicted to affect protein stability and 41/161 (25%) affect protein-protein interaction. These variants represent cases where use of a single structure may bias conclusions towards particular populations.

12. Exofacial membrane composition regulates plasma membrane P4-ATPase activity

Bartholomew P. Roland, T.R. Graham

The organization and composition of lipids within a cellular membrane directs their function. An important property of the plasma membrane is the asymmetric distribution of lipids on different sides of the bilayer. P4-ATPases, or flippases, translocate lipids from the exofacial- to the cytofacial side of the bilayer, and thus are the principal determinants of membrane asymmetry. Mutations within human P4-ATPase genes elicits cholestasis, metabolic disease, neurological dysfunction, and blood disorders. It is still unclear how these enzymes sort through the spectrum of lipids within their membrane environments to identify their desired substrate(s). We anticipate that competition for substrate binding and translocation occurs constantly, as these enzymes exist in a mixed environment of substrate and potential inhibitors/agonists. We used traditional pharmacologic examinations of a yeast plasma membrane P4-ATPase, Dnf2, to determine how P4-ATPases interact with the exofacial lipid environment. Next, we measured how substrate-specific changes in these P4-ATPases altered their sensitivities to the lipid environment. Finally, we directed membrane composition by manipulating lipid metabolism, thus

corroborating our exogenous inhibitor studies with endogenous adjustments of membrane composition. These experiments demonstrate a reciprocal enzymatic interaction between membrane composition and architecture that we propose is used to unify cellular lipid- and membrane homeostasis. Thus, we anticipate that P4-ATPases will be an exciting pharmaceutical target for the treatment of metabolic disease.

13. Microvillar sensation of shear stress induces autophagic flux in the intestinal epithelium

Sun Wook Kim, Jonathan Ehrman, Mok-Ryeon Ahn, Jumpei Kondo, Scott W. Crawley, Yun Sik Oh, Andrea Mancheno Lopez, James R. Goldenring, Matthew J. Tyska, Erin C. Rericha, Ken S. Lau

The intestinal epithelial cells lining the lumen of the neonatal gut are exposed to the flow of fluid from a liquid diet. Mechanosensors, such as the primary cilia of the kidney epithelium or stereocilia of the inner hair cell of the ear, have been identified to respond to shear forces. However, whether intestinal epithelial cells can respond to fluid shear stress is unknown.
To study the effect of shear on intestinal epithelial cells, we applied fluid shear stress on the intestinal epithelial cell line, Caco-2 BBE, through the use of a microfluidics design. Interestingly, we observed that exposure to fluid shear stress causes the formation of large vacuoles within intestinal epithelial cells when they are organized as monolayers. These observations raised two questions: first, what structural elements allow intestinal epithelial cells to transduce shear stress, and second, what mechanisms support the formation of large vacuoles that can exceed 80% of cell volume. As a result, we found that structurally, intestinal epithelial microvilli play a role in sensing extracellular shear stress, since shear-induced vacuole formation was significantly diminished when the intestinal microvilli were experimentally reduced. In addition, we identified that autophagic flux, and not endocytosis, to be the major pathway connecting mechanical sensation to vacuole formation. Loss-of-function studies by pharmaceutical and genetic inhibition of autophagy pathway components support our observations that shear stress-induced vacuole formation is mediated by the autophagic machinery.
In conclusion, our results revealed a novel link between the intestinal microvilli, the macroscopic transport of fluids across cells, and the autophagy pathway in organized epithelial monolayers. Our study contributes to the understanding of how physical stress affects cellular response in both intestinal physiological and pathological contexts.

14. Determination of cap cell fate in the developing mammary gland by lineage tracing

Armelle Le Guelte and Ian Macara

The participation of multipotent mammary stem cells (MaSC) in mammary gland morphogenesis remains controversial. Prospective enrichment using generic markers demonstrated the existence of MaSC in the context of a transplantation/regeneration assay. However, no markers were described that uniquely identified this population of cells. Lineage tracing with a Keratin-14 (K14) promoter, which is expressed in all the basal cells of the mouse mammary gland, failed to detect a multipotent stem cell population in postnatal glands. This result was later questioned by lineage tracing with a Keratin-5 (K5) promoter, which also marks

basal cells, and another paper claimed that rare ProCR$^+$ cells in the ducts were multipotent. However, ProCR$^+$ cells do not proliferate rapidly and likely provide only a limited contribution to mammary gland homeostasis.
The s-SHIP promoter was found to be active in multiple embryonic and tissue stem cells. The Rohrschneider laboratory created a transgenic mouse that expresses GFP from the s-SHIP promoter. GFP is expressed in several stem cell compartments and also in the cap cells at the tips of mammary Terminal End Buds (TEBs) during puberty. At the end of puberty s-SHIP is down regulated but is re-expressed in alveoli during pregnancy. These cap cells are negative for K14 and K5, and are also negative for luminal markers such as E-cadherin. Importantly, these cells can efficiently regenerate complete mammary glands after transplantation.
We show that tissue sections of the s-SHIP-GFP mammary glands have equally parallel and perpendicular divisions of the GFP+ cap cells in TEBs, suggesting that they might give rise to both myoepithelial and luminal body cells in the TEB. To evaluate the stemness of the s-SHIP$_+$ cells in situ, I created a new lineage tracing mouse line in which the 11.5 kb s-SHIP promoter drives expression of a mERCre(NLS)-mER fusion protein (MerCreMer), which exhibits Cre recombinase activity only in the presence of tamoxifen. The progeny were crossed to a floxed-STOP-tdTomato mouse. Unexpectedly, our in vivo data show that s-SHIP$^+$ cells give rise to only myoepithelial cells during puberty and pregnancy. However, cells isolated from these mice and cultivated in vitro can give rise to both myoepithelial and luminal cells populations. Moreover, specific ablation of s-SHIP$^+$ cap cells by Diphtheria toxin (DTA) expression suppresses mammary duct formation during puberty. Therefore, these cells do not normally function as multipotent stem cells in situ, but are essential for mammary gland development, and can be reprogrammed to express their stem cell fate when isolated from mice and either grown in vitro or transplanted into recipient mice. We are currently seeking the signaling pathways and transcription network that regulates the switch from myoepithelial progenitor to multipotent stemness in this population of cap cells.

---

15. Sphingolipids modulate the coordination of growth and cell wall formation in yeast

Marcin Wos and Kathleen L. Gould

Lipids containing a sphingosine backbone take part in multiple intracellular and intercellular signaling pathways. Disruption of signaling pathways mediated by sphingolipids are the origin of very severe neurodegenerative and metabolic disorders in humans. Through our study of a cytokinesis mutant, we have found that in the yeast, *Schizosaccharomyces pombe,* defects in sphingolipid metabolism uncouple growth from cell wall synthesis and cell division. Coupling cell wall construction with cell growth is a universal challenge for all walled organisms such as yeast, plants, and bacteria.
Css1 is an integral plasma membrane protein with phospholipase C and neutral sphingomyelinase activity. It cleaves the polar head group of sphingolipids, leaving ceramide. In strains conditionally mutant for Css1, cells cease growth and division and accumulate massive amounts of cell wall material at previous sites of growth. This phenotype can be partially suppressed by mutations in any one of three enzymes that produce cell wall constituents ags1, bgs1, bgs4, indicating that sphingolipid metabolites do not affect cell wall synthesis per se.
The sphingolipid biosynthesis pathway in *S. pombe* is very poorly understood. However, drugs that inhibit conserved enzymes acting early in sphingolipid biosynthesis and mutation of other enzymes acting early in the pathway suppress the *css1-3* temperature-sensitive phenotype.

These results are helping us to pinpoint the precise metabolite(s) whose increase uncouples growth from wall formation. We are constructing new gene mutations to help in this endeavor as well as employing mass spectrometry to identify metabolic intermediates.
Detailed investigation of sphingolipid synthesis will help us better understand this important pathway, signaling that lies behind it as well as its coupling with homeostatic cell growth.

16. Mammary myoepithelial cells respond to damage by altering cell fate in vivo

Lindsey Seldin and Ian Macara

Metastatic breast cancer is the second leading cause of cancer-associated deaths in women. Nevertheless, the molecular mechanisms underlying breast cancer initiation, metastasis and recurrence following chemotherapy remain poorly understood. The mouse mammary gland provides a robust mammalian system for investigating how epithelial behavior impacts tumorigenesis. The mammary epithelium is composed primarily of two lineage-restricted unipotent cell populations, an inner layer of milk-producing luminal cells and an outer layer of contractile myoepithelial cells. Nevertheless, despite their unipotent nature in situ, myoepithelial cells that have been cultured and passaged demonstrate a remarkable capacity to generate de novo mammary glands upon transplantation. We hypothesize that this distinction in myoepithelial plasticity between in vivo and culture conditions is mediated by a damage response. To test this hypothesis, we established an inducible transgenic mouse model that allows for in vivo lineage tracing of myoepithelial cells in the presence or absence of two distinct types of damage: mechanical damage and DNA damage. We find that upon mechanical damage, myoepithelial cells remain unipotent. Strikingly, however, myoepithelial cells become multipotent in response to DNA damage, giving rise to hyperproliferative luminal cells that cause aberrant luminal filling reminiscent of ductal carcinoma in situ (DCIS). Notably, this damage response has no effect on the structural integrity of the myoepithelial monolayer. These findings not only reveal a myoepithelial-specific DNA damage response that triggers cellular reprogramming, but also provide important insight into a potential cause of breast cancer recurrence following chemotherapy, a treatment that exploits DNA-damaging agents. These studies highlight the remarkable plasticity of mammary cell states. To determine whether this damage response is specific to mammary epithelium, we utilized a similar approach to test whether DNA damage would elicit cellular reprogramming in mouse epidermis. Remarkably, mouse epidermal progenitors become hyperproliferative and exhibit lineage infidelity, akin to our findings in the mammary gland. Important goals are to determine the molecular mechanisms that underlie this cellular plasticity and the unusual epithelial tissue response to DNA damage.
Supported by NCI grant R35 CA197571, NIH grant T32CA119925-08, NIH grant F32CA213794 DHHS.

17. F-actin is stabilized during differentiation

James Faust

The intestinal enterocyte undergoes a dramatic reorganization of the apical surface during differentiation as the cell transitions from the crypt to the villus. During the differentiation process filamentous actin (F-actin)-supported membrane protrusions known as microvilli are organized into a maximally packed highly ordered array of uniform length. Collectively, this ensemble of

microvilli is referred to as the brush border, and acts to increase the cell surface area for maximum nutrient absorption and host defense. Previous studies in the laboratory have begun to dissect the molecular mechanisms responsible for nucleation of F-actin within microvilli. However, little is known about regulation of F-actin assembly in the context of length uniformity. We analyzed the ability of F-actin to treadmill within brush border microvilli *in vivo* by applying cytochalasin or vehicle to the luminal surface of the intestine and measured length using structured illumination microscopy. At the villus, we observed no gross change in microvilli length *per se* for cytochalasin treated specimens compared to mock specimens indicating that F-actin within mature microvilli does not treadmill. At the base of the crypt we observed an ~50% reduction in microvilli length compared to mock specimens suggesting that, compared to the villus, F-actin in crypt microvilli are more dynamic. Surprisingly, we observed no overall change in fluorescence intensity at the apical surface along the crypt to villus transition between specimens. These data indicate that the transition from immature microvilli in the crypt to mature brush border microvilli is accompanied by stabilization of the underlying F-actin core bundle.

---

18. Non-random gamma-TuNA-dependent spatial pattern of microtubule nucleation at the Golgi

Anna A.W.M. Sanders, Kevin Chang, Xiaodong Zhu, Roslin Thoppil, William R. Holmes, and Irina Kaverina

Non-centrosomal microtubule (MT) nucleation at the Golgi generates MT network asymmetry in motile vertebrate cells. Investigating Golgi-derived MT (GDMT) distribution, we find that MT asymmetry arises from non-random nucleation sites at the Golgi (hotspots). Using computational simulations, we propose two plausible mechanistic models of GDMT nucleation leading to this phenotype. In the “Cooperativity” model, formation of a single GDMT promotes further nucleation at the same site. In the “Heterogeneous Golgi” model, MT nucleation is dramatically upregulated at discrete and sparse locations within the Golgi. While computationally both models are equally probable, GDMT nucleation leans toward simultaneous rather than sequential, supporting Heterogeneous Golgi model.

Investigating the molecular mechanism underlying hotspot formation, we have found that hotspots are significantly smaller than a Golgi subdomain positive for scaffolding protein AKAP450, which is thought to recruit GDMT nucleation factors. We have further probed potential roles of known GDMT-promoting molecules, including γ-TuRC-mediated nucleation activator (γ-TuNA) domain-containing proteins and MT stabilizers CLASPs. While both γ-TuNA inhibition and lack of CLASPs resulted in drastically decreased GDMT nucleation, computational modeling revealed only γ-TuNA inhibition suppressed hotspot formation.

We conclude that clustered GDMT nucleation is a result of γ-TuNA-dependent local activation of γ-TuRC at the Golgi.

---

19. Deciphering the bioactive chemical arsenal of myxobacterial predation

Caleb Fischer

Natural products are a diverse collection of small molecules produced by natural sources that form the backbone of most human therapeutics. Because of increasing antibiotic resistance and recalcitrant disease, additional chemical backbones are required. Novel strategies to unlock new

chemical diversity is an urgent need. Some groups of microorganisms encode numerous natural products yet only produce a small subset in traditional laboratory settings. Over the last decade, novel methodologies have addressed this shortcoming. One of these methods is to grow organisms in settings that mimic their natural ecologies, including growing them alongside competitor organisms.

Myxobacteria are a group of predatory microorganisms that encode numerous natural products. Despite consuming neighboring microorganisms in nature, all myxobacterial natural products discovered to date have come from strains grown in liquid monoculture. We hypothesized that growing myxobacteria in 'fight club' orientations—adjacent to prey microorganisms—would unlock additional small molecules. Moreover, a subset of these small molecules would be inhibitory toward the prey organism and could form the basis for new antimicrobial agents.

Here, we demonstrate that myxobacteria produce secondary metabolites specifically associated with predation. Using a combination of desorption electrospray ionization-imaging mass spectrometry (DESI-IMS) and bioautography imaging mass spectrometry (BIMS), we identify metabolites that are spatially localized to predation and that are inhibitory toward the prey organism. In sum, we show a novel method to help discover new bioactive small molecules in myxobacteria and present our preliminary findings.

---

20. Golgi-derived microtubules in pancreatic β-cells are regulated by glucose through cAMP and EPAC2

Kathryn Trogden, Guoqiang Gu, and Irina Kaverina

Insulin release from pancreatic β-cells is tightly regulated. In response to evenly sustained high glucose only a small fraction of insulin granules are released. Previous work from our lab has shown that microtubules (MTs) act to negatively regulate insulin release and in response to high glucose are destabilized to help with the release of granules. The formation of MTs in cells occurs primarily through templated nucleation, which uses the γ-tubulin ring complex as a template and can occur at the centrosome, from the side of previously formed MTs (augmin-dependent), or at the Golgi. Successful MT formation also requires stabilization of newly-forming MT seeds, a process that is known to require CLASP2 for Golgi-derived microtubules (GDMTs). Previous work has shown that GDMT nucleation in pancreatic β-cells is increased upon a high glucose stimulus. Now, we have addressed the function of these newly formed GDMTs. Our data indicate that they likely play a role in trafficking of newly synthesized proinsulin through the membrane networks from the ER to the Golgi and further into nascent secretory granules, and might affect proinsulin to insulin processing, potentially affecting glucose-stimulated insulin release (GSIS). We were also interested in what processes in the cell cause the increase in GDMTs in response to high glucose. Here we show that GDMT nucleation increases in two waves in response to high glucose in an isolated β-cell line, MIN6, which mirror the well-described two waves of GSIS. The first wave doubles to amount of GDMTs and occurs rapidly, peaking by 5 minutes. This increase proceeds the expansion of the Golgi that occurs during glucose stimulation, indicating it involves a change in regulation and not an increase in available sites for nucleation. We decided to further explore what is causing this increase during the first wave. We have found that the cAMP pathway, which is also involved in GSIS, controls the increase in GDMT nucleation. Addition of a cAMP analog in low glucose leads to a doubling of GDMT nucleation. Out of the two major cAMP effectors, EPAC2, a paralog of the more ubiquitously expressed EPAC1, rather than protein kinase A (PKA) cause this increase. Interestingly, EPACs interact with the light chain, LC2 and LC1, of MAP1A and MAP1B,

respectively, which are known to bind and stabilize MTs. We propose that EPAC2 in β-cells is acting though LC1 or LC2 to stabilize newly nucleated GDMTs. When activated upon glucose stimulation, EPAC2 stabilizes these the newly formed GDMTs allowing them to grow out from the template, therefore increasing the number of GDMTs in high glucose. To better understand this process, we are currently testing this hypothesis.

21. Optimization of Laser Capture Microdissection for Isolation of the Enteric Ganglia from Fresh-Frozen Human Tissue

Aaron A. May-Zhang, Karen K. Deal, E. Michelle Southard-Smith

Gastrointestinal and gut motility disorders affect one of every four people in the United States. The enteric nervous system (ENS), also referred to as the "second brain," is often at the center of these disorders, as it plays a crucial role in gut homeostasis and motility. Surprisingly, the full transcriptome of the adult ENS remains to be sequenced, greatly limiting our ability to identify molecules within the ENS that can be targeted pharmaceutically or utilized in stem cell therapies.

To catalog the diversity of genes expressed in the human ENS, we have begun collecting samples of enteric ganglia from normal human intestinal tissue using laser-capture microdissection (LCM). Isolation of RNA from fresh frozen tissue is fraught with potential complications that can compromise RNA integrity. Here, we highlight modifications to the LCM process that provide RNA of high yields and sufficient quantity for RNA-Seq.

22. MTGR1 regulates stem cell dynamics and protects against stress-induced stem cell failure

Sarah P. Short, Jing Wang, Yue Zhao, Bobak Parang, Yash A. Choksi, Scott W. Hiebert, Christopher S. Williams

Myeloid translocation gene related 1 (MTGR1) is a transcriptional corepressor highly expressed in the intestine. To investigate the role of MTGR1 in small intestinal biology, we intercrossed *Mtgr1*$^{-/-}$ mice with the *Lgr5-CreER-GFP* stem cell reporter mice and observed increased LGR5 (+) stem cells in the setting of MTGR1 loss. *Mtgr1*$^{-/-}$ mice also displayed increased proliferation and upregulation of stem cell markers such as *Lgr5* and *cMyc*. RNA-sequencing and gene set enrichment analysis further determined highly significant upregulation of metabolism-associated gene-sets in *Mtgr1*$^{-/-}$ crypts.

We next utilized a 3D intestinal organoid (enteroid) model to investigate stem cell function. As compared to WT, enteroids from *Mtgr1*$^{-/-}$ mice displayed a 2-fold increase in plating efficiency and a greater proportion of stem spheroids, indicating increased “stemness.” However, despite this initial expansion, *Mtgr1*$^{-/-}$ enteroids failed to generate crypt buds and rapidly died, with greater than 95% loss of viability by day 5 post plating. Loss of viability appeared due to stress-induced loss of proliferative cells, as 3-day-old *Mtgr1*$^{-/-}$ enteroids displayed decreased Ki67 staining and downregulation of intestinal stem cell markers such as *Lgr5* and *Olfm4*. Stem cell loss was not associated with apoptosis, and instead *Mtgr1*$^{-/-}$ enteroids appeared poised toward cell cycle exit and commitment differentiation, with over 2-fold increases in several cyclin dependent kinase inhibitors and enrichment for markers of differentiated enterocytes. Taken together, these data indicate MTGR1 loss induces stem cell expansion in the setting of

homeostasis, yet leads to stem cell failure and aberrant differentiation in the setting of proliferative stress.

23. CLASP1 is Required for CLASP2 Localization and Function at Microtubules in Interphase Cells

Roslin J. Thoppil, Anna A.W.M Sanders, Elizabeth J. Lawrence, Kevin Chang, Shwetha Narasimhan, Marija Zanic and Irina Kaverina

CLIP-associated proteins (CLASPs) are highly conserved microtubule (MT) plus-end tracking proteins (+TIPs) that are involved in regulating MT dynamics; specifically, CLASPs were shown to promote MT rescue and enhance MT stability. Human CLASPs consists of two paralogs: CLASP1 and CLASP2, which have been found associated with the cell cortex, kinetochores, the Golgi and at the ends of growing MTs. Although both CLASPs have been structurally and functionally characterized in depth, mutual regulatory interactions between these two proteins have not been explored. In the present study, we use a variety of human cell lines to show that while CLASP2 depletion does not interfere with cellular CLASP1 localization, the loss of CLASP1 dramatically influences CLASP2 localization in interphase. In particular, CLASP2 is no longer associated with MT plus ends, while other MT +TIPs were not affected, and CLASP2 still retained at the Golgi. This effect suggests that CLASP1 specifically facilitates CLASP2 localization at the MT plus ends. Addressing potential underlying mechanisms, we tested if CLASP1 was involved in regulating CLASP2 phosphorylation by GSK3β, which is known to abolish CLASP2 binding to MTs. Here, we found that CLASP1 did not modify CLASP2 phosphorylation levels. Moreover, when GSK3β was inhibited in CLASP1-depleted cells, CLASP2 localization to MTs was restored, indicating that CLASP1 is capable to localize CLASP2 to MTs despite its physiological phosphorylation level. Moreover, our co-immunoprecipitation assays show that CLASP1 forms a complex with CLASP2 in cells. Since prior evidence indicates that CLASP variants can homodimerize via a C-terminal coiled-coil region, we propose that CLASP1 heterodimerizes with CLASP2 in order to target it to MTs. Functionally, CLASPs play a prominent role in MT dynamics and stability, and are critical for nucleation of Golgi-derived microtubules (GDMTs). In our in vitro reconstitution assays, CLASP2 by itself strongly promotes MT nucleation. However, decrease of GDMT nucleation in cells depleted of CLASP1 alone was as prominent as the effect of depletion of both proteins. We conclude that CLASP1-dependent localization of CLASP2 to MT ends is necessary for CLASP2 function in cells, and thus CLASP1 is upstream of CLASP2 in regulating MT nucleation and dynamics.

24. Identification of maximally predictive models of signal transduction pathways

Hossein Jashnsaz, Zachary Fox, Guoliang Li, Brian Munsky, and Gregor Neuert

A hallmark of life is organisms' ability to maintain homeostasis under external and internal perturbations. However, the mechanisms of how cells sense, process, and respond to extracellular stress are not yet fully understood. Therefore, cell signaling response upon environmental changes that change over time or genetic mutations is not predictable. We develop a combined theoretical and experimental framework that will enable us to ultimately build predictive models of signal transduction networks for any pathway, in any organism, and in any environmental condition. We built our model based on a prior signal transduction pathway

topology. At its core it is an n-node circuit motif, a network of n interacting signaling proteins, where each node in principle could regulate other nodes thorough activation or deactivation functions. To demonstrate the feasibility of our approach, we use the High Osmolarity Glycerol (HOG) Stress Activated Protein Kinase (SAPK) signaling pathway in the yeast *Saccharomyces cerevisiae* model system. Under various experimental extracellular temporally changing osmolyte profiles (e.g., step, pulse, ramp, and quadratic over time), Hog1 signaling duration, intensity, and shape show distinct responses. For example, constant osmolyte ramp rate with different durations results in constant Hog1 signaling intensity. Increased osmolyte rate of fixed duration correlates with Hog1 signaling intensity. And, quadratic increase in the external osmolarity linearly increases Hog1 nuclear enrichment. As future direction, we will apply our systematic fitting-prediction approach on Hog1 response data to iteratively design optimal environmental perturbations (as well as mutation experiments) that will ultimately enable us in optimal model selection.

25. Human CLASP2 specifically regulates microtubule catastrophe and rescue

Lawrence EJ, Arpag G, Norris S and Zanic M

Cytoplasmic Linker-Associated Proteins (CLASPs) are microtubule-associated proteins essential for cell division, migration and neuronal development. In cells, CLASPs regulate microtubule dynamics, however, the molecular mechanisms underlying CLASP activity are not understood. Here, we use purified protein components and Total Internal Reflection Fluorescence (TIRF) microscopy to investigate the effects of human CLASP2 on microtubule dynamics *in vitro*. We demonstrate that CLASP2 suppresses microtubule catastrophe and promotes rescue without affecting the rates of microtubule growth or shrinkage. Strikingly, when CLASP2 is combined with EB1, a known binding partner, the effects on microtubule dynamics are strongly enhanced. We show that synergy between CLASP2 and EB1 is dependent on a direct interaction, since a truncated EB1 protein that lacks the CLASP2-binding domain does not enhance CLASP2 activity. Further, we find that EB1 targets CLASP2 to microtubules and increases the dwell time of CLASP2 at microtubule tips. Although the temporally averaged microtubule growth rates are unaffected by CLASP2, we find that microtubules grown with CLASP2 display greater variability in growth rates. Our results provide insight into the regulation of microtubule dynamics by CLASP proteins and highlight the importance of the functional interplay between regulatory proteins at dynamic microtubule ends.

26. SELECTIVE AUTOPHAGY: A MECHANISM FOR CYTOPLASMIC ANTIGEN PRESENTATION BY MHC CLASS II MOLECULES

Naveen Chandra Suryadevara, Amrendra Kumar, Pavlo Gilchuk, Timothy M. Hill, & Sebastian Joyce

The prevailing view suggests that macroautophagy delivers cytoplasmic antigens to the endo/lysosomes for presentation by MHC class II molecules. Contrary to the prevailing view, we found that the male HY alloantigen and to some extend the listerolysin O antigen of *Listeria monocytogenes*, were intact in mice deficient in Atg5-dependent macroautophagy. This finding suggested that another mechanism is operative for delivering certain cytoplasmic antigens to the endo/lysosomes. Chaperone mediated autophagy (CMA) is a cellular stress response, which

selectively delivers cytoplasmic proteins to lysosomes for degradation, and is known to deliver cytoplasmic antigens to the endo/lysosomes. CMA is initiated by the recognition of a KFERQ motif by heat shock cognate chaperone of 70kD (Hsc70), which tethers to LAMP2 and induces its oligomerization into a transmembrane pore. Curiously, however, neither LAMP2 nor Hsc70 are NTP hydrolases, which leaves open the source of energy for peptide translocation across the endo/lysosomal membrane. Recent studies have shown that an orphan TAP (transporter-associated with antigen processing)-like protein and a member of the ABC family can transport cytoplasmic peptides into model vesicles. Hence, we postulated that TAP-L may participate in CMA especially of substrates lacking the KFERQ motif. As the first step in testing this postulate, we found that mouse TAP-L associates with mouse and human LAMP2 as does human TAP-L with human LAMP2 and Hsc70. This finding foretells a potential role for TAP-L in CMA, the mechanism of which is currently under investigation.

---

27. Inflammatory factors drive the molecular etiology of pulmonary arterial hypertension in KCNK3$^{-/-}$ mice

Anandharajan Rathinasabapathy

Rationale

Loss of function of KCNK3 gene has been recently identified to drive pulmonary arterial hypertension (PAH) in human. Metabolic or vasoconstrictive or inflammatory defects trigger the onset of heritable or idiopathic PAH. However, the mechanism which triggers PAH in KCNK3$^{-/-}$ animals is unknown.

Methods

Tamoxifen-inducible ubiquitin-CRE mice x double floxed KCNK3 or controls were induced recombination. To assess the impact of vasoreactivity or metabolism/long-term hematopoiesis or inflammation, animals were exposed to 10% normobaric hypoxia or high-fat diet or lipopolysaccharide, respectively. Mice underwent hemodynamic phenotyping, complete blood counts, bone-marrow flow-sorting, α-smooth muscle actin (α-SMA) staining, western blotting of CD3ε, CD45 and CD68, and cytokine array analysis.

Results

Hemodynamic phenotyping demonstrated that vasoconstrictive or metabolic defects did not affect right ventricular systolic pressure (RVSP). However, RNA-seq studies demonstrated that inflammatory markers (SAA1, GDF15, Ptk6, Adamts17, Disc1 and Csf2) were upregulated in KCNK3$^{-/-}$ animals. Flow sorting suggested that multipotent and ST-HSC cells were significantly upregulated in KCNK3$^{-/-}$ mice and ST-HSCs increase significantly correlated with circulating monocytes and macrophages. In presence of LPS, RVSP and RV weight was significantly increased in KCNK3$^{-/-}$ animals. These resulted a significant pulmonary vascular remodeling (α-SMA), 2x increase in CD3ε, CD45 and CD68 (western blotting) and elevated expression of CXCL13, SDF1, RANTES, and CXCL9 (cytokine array) in KCNK3$^{-/-}$ lungs.

Conclusions

Knocking out of KCNK3 leads to pulmonary and bone-marrow inflammation. Specific stimulation of inflammatory signals with LPS developed PAH, pulmonary vascular and RV remodeling suggesting, inflammatory stress predominantly drive PAH in KCNK3$^{-/-}$ animals.

28. Comparable calcium handling and contractility in human iPSC cardiomyocyte models of three different hypertrophic cardiomyopathy-linked mutations

Kyungsoo Kim, Lili Wang, Vasco Sequeira, Joseph C. Wu, Bjorn C Knollmann

Familial hypertrophic cardiomyopathy(HCM) is caused by mutation of sarcomere genes which is associated with an increased risk of sudden cardiac death due to arrhythmia. Sarcomere gene mutations typically disrupt the highly tuned balance between force generation and calcium(Ca) cycling dynamics. Here we investigated the relationship between Ca handling and contractility properties in human induced pluripotent stem cells(hiPSC) derived cardiomyocyte(CM) of three different HCM-linked mutations (Troponin T I79N: TnT–I79N, Troponin T K280N: TnT–K280N, and Myosin heavy chain7 R663H: MHC7–R663H). We generated hiPSC lines from healthy donors and two TnT mutations (TnT–I79N and TnT–K280N) using CRISPR/Cas9. The Matrigel mattress method was used to generate single rod-shaped cardiomyocytes and measured Ca transients and contractility at field-stimulation (0.2 Hz) in Fura-2, AM loaded iPSC-CMs. In response to the pacing stimulus, all HCM mutations significantly increased the percentage of cell shortening. The time to peak of shortening was not changed, whereas relaxation time was significantly prolonged in comparison to their isogenic controls. Although the properties of force generation were similar in all HMC-linked mutations, their Ca handling was quite different. In TnT–I79N and TnT–K280N mutations, despite the reduced or unchanged Ca amplitude, they exhibited both enhanced contractility and delayed relaxation, indicative of increased sensitivity to Ca. However, in MHC7-R663H mutation, albeit consistent hypercontractility and impaired relaxation similar to other two HCM mutations, Ca amplitude as well as diastolic Ca significantly increased, which reflects the possibility of unchanged sensitivity of the myofilaments to Ca. Although further studies need to focus on elucidation of how different Ca handling defect causes common HCM phenotype in these HCM-related mutations, our findings robustly demonstrated key features of HCM (i.e., increased systolic and impaired diastolic function) in various HCM-linked hiPSC-CM mutations using measurement of contractile and cytosolic Ca.

29. Evolutionary rewiring of the genetic regulatory network controlling spore formation in filamentous fungi

Matthew Mead

The formation of spores is a key factor contributing to the survival and fitness of many fungi. Properly assembled spores allow fungi to endure stressful conditions and disperse to new environments such as plant leaves and human lungs. Spore formation is controlled by a complex gene regulatory network (GRN) that affects a variety of other processes. To gain mechanistic insights into how fungal sporogenesis is controlled across species, we dissected the GRN downstream of a major regulator of spore maturation (*wetA*) in three *Aspergillus* species that span the diversity of the genus: the genetic model *A. nidulans*, the human pathogen *A. fumigatus*, and the plant pathogen *A. flavus*. RNA sequencing of *wetA* null mutant and wild-type spores showed that while the biological processes controlled by the *wetA* GRN are very similar across the three species, the underlying list of genes that function during those processes and are regulated by *wetA* are vastly different. This suggests that network rewiring has occurred during the evolution of spore formation in *Aspergillus*. To gain insight into how this rewiring may

have occurred, we carried out ChIP-seq experiments in *A. nidulans* that identified a potential WetA binding site whose sequence is completely conserved throughout *wetA* orthologs in *Aspergillus*. Further analysis of our ChIP-data suggested that the rewiring of the *wetA* network occurred via the gain and/or loss of the potential binding site in specific genes. Our results indicate that gene network rewiring is more common in filamentous fungi than previously acknowledged.

---

30. Scavenging reactive aldehydes with 5'-O-pentyl-pyridoxamine (PPM) improves HDL function and reduces atherosclerosis in Ldlr deficient mice

Jiansheng Huang, Linda S. Zhang, Patricia G. Yancey, Huan Tao, Lei Ding, Youmin Zhang, John A. Oates, Venkataraman Amarnath, L. Jackson Roberts II, Sean S. Davies, MacRae F. Linton

Background: Lipid peroxidation products impair the cholesterol efflux capacity of high-density lipoprotein (HDL) and contribute to the development of atherosclerosis. The effect of inhibition of HDL dysfunction by scavengers on HDL function and whether scavenging reactive aldehydes with PPM protects against the development of atherosclerosis was examined.
Methods and Results: HDL of familial hypercholesterolemia (FH) subjects have impaired ability to promote cholesterol efflux and FH-HDL contain 5-fold more malondialdehyde adducts (MDA) than control HDL. In vitro studies revealed that reactive aldehyde malondialdehyde (MDA) crosslinks apolipoprotein AI (apoAI) and impairs the ability of HDL to promote cholesterol efflux from *Apoe*$^{-/-}$ macrophages in a MDA dose dependent manner. Western blot analysis of apoAI revealed that 5'-O-pentyl-pyridoxamine (PPM), a potent scavenger of reactive aldehydes, abolished MDA-mediated crosslinking of apoA-I in HDL (molar ratio of MDA and HDL is 1:5) by 80 % ($P<0.05$). PPM prevents the reduction in cholesterol efflux capacity of MDA treated HDL in Apoe-/- macrophages. Furthermore, PPM significantly improved the cholesterol efflux capacity of HDL from *Ldlr*$^{-/-}$ mice fed a Western diet (WD) for 16 weeks ($P<0.05$), indicating that PPM protects HDL from modifications by reactive aldehydes and maintains HDL function in vivo. Importantly, administration of 1 mg/mL of the reactive aldehyde scavenger PPM, versus 1 mg/mL of the nonreactive analogue PPO, to *Ldlr*$^{-/-}$ mice consuming a WD for 16 weeks reduced the extent of proximal aortic atherosclerosis by 45% ($P<0.05$). Immunohistochemistry studies revealed that PPM reduced the macrophage content and the number of TUNEL positive cells by 55% ($P<0.05$) and by 60% ($P<0.01$) in advanced atherosclerotic lesions of *Ldlr*$^{-/-}$ mice, respectively. In addition, the necrotic core area was reduced by 52% ($P<0.05$) in advanced atherosclerotic lesions in *Ldlr*$^{-/-}$ mice treated with PPM compared to the control group.
Conclusions: Treatment with PPM, a reactive aldehyde scavenger: 1) inhibits MDA-ApoA1 adduct formation thereby preserving HDL cholesterol efflux capacity; 2) improves the ability of HDL to promote cholesterol efflux in *Ldlr*$^{-/-}$ mice fed on a WD for 16 weeks; 3) reduces the macrophage content and the number of apoptotic cells in atherosclerotic lesions of *Ldlr*$^{-/-}$ mice; 4) decreases the necrotic core area in lesions of *Ldlr*$^{-/-}$ mice. These results support the therapeutic potential of PPM in the treatment of atherosclerotic cardiovascular disease.

Keywords: Cholesterol efflux, high-density lipoprotein (HDL), Malondialdehyde (MDA)

31. Improved calcium handling in human induced pluripotent stem cell cardiomyocytes

Daniel Blackwell

Human induced pluripotent stem cell cardiomyocytes (hiPSC-CM) are being increasingly used to model cardiac disease. However, investigation of calcium handling and arrhythmias has been hampered by lack of t-tubule development and poor calcium-induced calcium release (CICR). We recently developed a hormone maturation protocol (addition of T3, Dexamethasone, and Matrigel substrate) that promoted t-tubule genesis in hiPSC-CM. To investigate whether calcium handling was improved in these cells, we utilized a saponin-permeabilized cell spark assay to measure sarcoplasmic reticulum (SR) calcium release via the ryanodine receptor (RyR2). Hormone-treated cells showed a significant improvement in the frequency of calcium release, time to peak, and the amount of calcium released as assessed by spark mass, without altering total SR calcium content. Notably, these values were similar to those observed in isolated mouse ventricular cardiomyocytes, indicating mature RyR2 clustering and localization. To examine this, we performed immunostaining of RyR2 and found that our hormone-treated hiPSC-CM had a striated pattern consistent with dyadic localization, in contrast to diffuse perinuclear staining from vehicle-treated hiPSC-CM. We electrically paced hiPSC-CM and found that our maturation method significantly improved the uniformity of calcium release, indicating that the t-tubules functionally connect the L-type calcium channel with RyR2 calcium release throughout the cell. These results were also verified in a second hiPSC line, suggesting that we can mature hiPSC-CM to improve calcium handling and calcium release properties. Our maturation method provides a good model for examining cardiac arrhythmias and calcium release in human cardiomyocytes.

32. Human T1D and T2D pancreatic islets have a higher number of lipid-rich droplets than surrounding pancreatic acinar cells

Xin Tong, Chunhua Dai, Al Powers and Roland Stein

Our groups have shown by electron microscopy that transplanted human islets, compared to mouse, appear to have a much higher capacity to form lipid droplets. We hypothesize that the high lipid-rich droplets (LD) content of human islets contributes to their relative unresponsiveness to proliferation and secretion signals in comparison to mouse. Consequently, we used both electron microscopy and the Bodipy 493/503 dye to analyze LD content in various human and mouse pancreatic contexts. We observed that Bodipy LD signals were: 1) essentially only observed in human pancreatic samples, and not mouse; 2) apparently randomly distributed between the acinar and endocrine compartments in healthy pancreas (n=4); and strikingly, 3) enriched within T2D (n=10) and longstanding T1D (n=2) islets in relation to their acinar space. We found the Bodipy signals involve the LD-associated proteins PLIN2 and PLIN3, the principal perilipin members expressed in human islets by transcriptome and immunofluorescent staining analysis, while all family members were produced at much lower levels in mouse islets. To obtain mechanistic insight into the contribution of PLIN2 and 3 in LD formation, we are analyzing how reduction in protein levels impacts exogenous lipid-induced LD formation in the human β cell line, EndoC βH2 cells. Taken together, these early observations suggests a unique capacity of human (likely vertebrate) islets to form LD, which might contribute to the a) differences observed

between human and mouse in their response to mitogenic and metabolic signals; b) islet α cell dysfunction in T1D and α and β in T2D.

33. Molecular Assessment of Antimalarial Drug Resistance Using Sentinel L-DNA Thermal Probes

Mindy Leelawong, Nicholas Adams, Rick Haselton, David Wright

Polymerase chain reaction (PCR) is the gold standard laboratory-based diagnostic for many infectious diseases. Although PCR is a more sensitive alternative to traditional malaria detection methods, its complexity prevents it from being more widely disseminated. Our group has developed a new PCR platform that circumvents an essential but limiting function of thermal cyclers: temperature monitoring. Our improved design, now known as Adaptive PCR, uses mirror-image L-DNA molecules that serve as sentinels to control the two temperature-dependent steps: template denaturation and primer annealing. The sentinel L-DNAs exhibit thermodynamic properties identical to conventional DNA, but they do not participate or interfere with enzymatic reactions. Therefore, neither temperature measurements nor machine programming are required. Instead, the device fluorescently evaluates L-DNA denaturation and annealing to trigger switching between heating and cooling. The ability of the Adaptive PCR instrument to self-adjust based on the sample composition provides greater flexibility with the reaction components. As a proof of concept, we have exploited this platform to detect a single nucleotide polymorphism associated with chloroquine drug resistance in the malaria parasite *Plasmodium falciparum*. We can reliably differentiate between chloroquine sensitive and resistant parasites based on the detection of a key point mutation in the chloroquine resistance transporter (*pfcrt*) gene. These findings will be further expanded to include other molecular markers of drug resistance.

Keywords
Drug resistance
Molecular diagnostics
Plasmodium falciparum
Polymerase chain reaction (PCR)

34. Gene Function Analysis of Alzheimer's Genetic Risk Factor Phospholipase D3

AG Nackenoff, Ph.D. & MS Schrag, M.D./Ph.D.

Alzheimer's disease is the most common form of dementia, and represents a large and increasing societal and economic burden. Recently, a highly-penetrant familial gene variant was discovered in the Phospholipase D3 (PLD3) gene[1], which is not directly known to impact canonical β-amyloid pathways. Studying highly penetrant disease associated gene variants allow us to discern previously hidden novel causative mechanisms. We aim to discern previously unidentified gene function and localization with respect to Alzheimer's disease pathology.

In transient transfection systems, 5xFAD mouse model, and Alzheimer's disease associated tissue, PLD3 localizes in lysosomes (confirmed via counterstaining with lysosomal markers LAMP1 and Cathepsin B). In disease relevant tissue, PLD3 is upregulated around β-

amyloid plaques, remaining in lysosomes, though these lysosomes appear severely enlarged. While the lysosomes maintain ubiquitous LAMP1 expression across various sized β-amyloid plaques, the protease Cathepsin B does not. This suggests that as the β-amyloid plaque increases in size and burden, these lysosomes become functionally impaired.

In enzyme assays following PLD3 transient overexpression, purification, and pulldown, PLD3 appears not to be functional as a phospholipase at physiologic pH. When we analyze enzymatic activity in isolated lysosomes, or at lysosomal acidic pH, PLD3 appears to be functional as a phospholipase, Furthermore, human associated Alzheimer's disease associated variant and proposed inactivating mutations render PLD3 non-functional as a phospholipase, regardless of pH.

Further experimentation is being performed to establish whether these enlarged lysosomes around amyloid plaques fail to acidify, which would impact PLD3 functionality, and whether re-acidification would repair lysosome functionality and thus reduce plaque burden.

1. Cruchaga, C. *et al.* Rare coding variants in the phospholipase D3 gene confer risk for Alzheimer's disease. *Nature* **505,** 550–554 (2013).

35. Circulating transfer RNA-derived small RNAs are altered in patients with rheumatoid arthritis

Qiong Wu, Quanhu Sheng, Joseph F Solus, Kasey C Vickers, Ryan Allen, Shilin Zhao, Yan Guo, Fei Ye, C Michael Stein, Michelle J Ormseth

Small RNAs (sRNAs) are important gene regulators and markers of disease. Transfer RNA (tRNA)-derived sRNAs (tDRs), including tRNA fragments (tRFs) and halves (tRHs), are novel regulatory sRNAs, which are often upregulated in cellular stress to downregulate metabolic processes. Rheumatoid arthritis (RA), a common autoimmune disease, is associated with excessive cellular stress due to immune activation. We hypothesized that circulating tDRs are altered in RA patients and serve as novel markers for RA and disease activity. To test this sRNA sequencing was performed on archived plasma samples from 167 RA patients and 91 matched controls using Illumina NextSeq500. tDRs were quantified by TIGER pipeline, permitting one mismatch. Total tDRs, individual tDR sequences and tDRs based on amino acid of the parent tRNA normalized to total reads were compared between RA and control subjects by DESeq2 with adjustment for age, race, sex, and batch with 5% false discovery rate adjusted by Benjamini-Hochberg method. RA patients had 1.16-fold higher proportion of total plasma tDRs compared to controls. Among RA patients a higher proportion of total plasma tDR reads was associated with higher disease activity by DAS28 score (Rho=0.17, p=0.03), erythrocyte sedimentation rate (Rho=0.21, p=0.007) and swollen joint count (Rho=0.18, p=0.02). Seven individual tDR sequences were increased (3.7-fold to 1.5-fold), and one individual tDR sequence was decreased 2.2-fold among RA patients. tDRs from a suppressor tRNA were increased 1.7-fold, and tDRs from tRNAs encoding for asparagine, isoleucine, and aspartic acid were decreased (1.8-fold to 1.5-fold) among RA patients. These data show that RA patients have a greater proportion of plasma tDRs compared to controls, and total tDRs were correlated with disease activity. Several individual tDR sequences, and tDRs from a suppressor tRNA and several other parent tRNAs were altered in RA patients. Circulating tDRs may be novel markers of RA and disease activity.

36. Selection of Optimal Myometrial Cells for High-Throughput Screening for Novel Regulators of Uterine Contractility

Shajila Siricilla, PhD, Kelsi Knapp, Jennifer Condon, PhD, Dehui Mi, PhD, Paige Vinson, PhD, Bibhash C. Paria, Jeff Reese, MD, Jennifer Herington, PhD.

Introduction: The uterine myometrium (UT-myo) is a therapeutic target for regulating uterine contractions. A final pathway controlling myometrial contractions involves stimulation of intracellular calcium [Ca_{2+}]i-release. Therefore, we developed an assay for high-throughput screening (HTS) of small-molecules to regulate Ca_{2+}-mobilization in UT-myo cells. In order to select the optimal UT-myo cells for our drug discovery assay, we compared the gene expression of contraction-associated proteins (CAPs) as well as functional response to oxytocin (OT) between: 1) term-pregnant human and mouse myometrial tissue, 2) isolated primary human and mouse UT-myo cells, 3) commercially-available pregnant human myometrial (PHM1) cells and 4) human telomerase immortalized (hTERT) myometrial cells.
Methods: Primary human and mouse UT-myo cells were isolated from tissue collected at the time of c-section during term pregnancy (≥37 weeks or 19 days, respectively). Quantitative RT-PCR was used to determine the gene expression levels of CAPs: OT-receptor, prostaglandin F receptor and connexin-43. Cell density and passage number (low and high) were optimized, and cell viability was monitored for each automated step used during the 384-well format HTS Ca_{2+}-mobilization assay. Thirteen-point, 3-fold dilutions of OT were tested in the Ca_{2+}-mobilization assays, followed by calculations of the OT EC_{50} and %induction, to determine the responsiveness and sensitivity of myometrial cells. Finally, data were analyzed by 1-way ANOVA.
Results: The relative mRNA expression levels of CAP genes were significantly ($p<0.05$) less in all four myometrial cell types examined compared to endogenous levels measured from human tissue. However, the mRNA expression of CAP genes in PHM1 and hTERT cells were similar to that measured from primary human myometrial cells. Moreover, PHM1 and hTERT cells were more responsive to OT-induced [Ca_{2+}]i-release (EC_{50} = 60nM and 40nM, %induction = 200% and 70%, respectively) compared to human and mouse primary myometrial cells.
Conclusion: While there is a benefit of using primary cells in HTS due to their retention of many *in vivo* functions and endogenous expression of mechanisms/targets of interest, primary cells must be proven reproducible for reliable use in HTS and available at similar robust numbers to that of cell lines. Among the 4 different myometrial cells examined, both PHM1 and hTERT cells exhibit similar gene expression levels of CAPs found in primary isolated cells from term pregnant human myometrial tissue, and are the most responsive to OT-induced [Ca_{2+}]i-release.

37. DNA methylation quantitative trait loci and breast cancer risk: an analysis of data from nearly 230,000 women of European descent

Yaohua Yang, Qiuyin Cai, Xiao Ou Shu, Xiang Shu, Lang Wu, Bingshan Li, Xingyi Guo, Fei Ye, Kyriaki Michailidou, Manjeet K. Bolla, Qin Wang, Joe Dennis, Jacques Simard, Douglas F. Easton, Wei Zheng, Jirong Long

Background and Objective: DNA methylation plays a critical role in the development of cancers including breast cancer. Previous studies have identified several promising methylation

markers associated with breast cancer risk. However, these studies are limited by small sample sizes and potential confounding effects.

Material and Methods: We used methylation quantitative trait loci (meQTL) single nucleotide polymorphisms (SNPs) as instruments to investigate 30,477 CpG sites (CpGs) in association with breast cancer risk using data from 122,977 breast cancer cases and 105,974 controls included in the Breast Cancer Association Consortium (BCAC). For the CpGs associated with breast cancer, we attempted to identify genes whose expression levels are correlated with methylation levels using data from the Framingham Heart Study (FHS). For genes with expression correlated with breast-cancer-risk-associated CpGs, we built expression prediction models via genetic variants using data from the Genotype-Tissue Expression (GTEx) project and then applied them to the BCAC data to evaluate the association of predicted gene expression level and breast cancer risk.

Results: Of the 30,477 CpGs investigated, significant associations with breast cancer risk were observed for 199 CpGs at $P < 1.64\times10^{-6}$, a Bonferroni-corrected threshold. Among them, 22 CpGs were located in genomic regions not yet reported for breast cancer. Of the 177 CpGs located in known breast cancer risk loci, 19 were associated with breast cancer risk independently of previously identified genetic variants. Methylation levels at 28 CpGs were correlated with expression level of 17 genes, of which ten genes were significantly associated with breast cancer risk.

Conclusion: We identified 199 CpGs and ten genes significantly associated with breast cancer risk, providing new insights into breast cancer genetics and biology.

---

38. RNA interference efficiently targets human leukemia driven by a fusion oncogene in vivo.

Nidhi Jyotsana

Efficient and safe delivery of siRNA in vivo is the biggest roadblock to clinical translation of RNA interference (RNAi) based therapeutics. To date, lipid nanoparticles have shown efficient delivery
of siRNA to the liver; however, delivery to other organs, especially hematopoietic tissues still remains challenging. We developed DLin-MC3-DMA lipid-based nanoparticle (LNP)/siRNA formulations for systemic delivery to human B-cell acute lymphoblastic leukemia (ALL) cells in vivo. A microfluidic mixing technology was used to obtain reproducible ionizable cationic lipid nanoparticles (LNPs) loaded with siRNA molecules targeting TCF3-PBX1 fusion oncogene, one of the most frequent translocation in pediatric and adult B-ALL. We show a highly efficient and non-toxic delivery of siRNA in vitro and in vivo with up to 90% uptake of LNP-siRNA formulations in bone marrow of leukemia patient derived xenograft B-ALL model. By targeting TCF3-PBX1 fusion oncogene we show an improved survival of ALL mice compared to control siRNA treated mice mediated by target knockdown. Our study provides proof-of-principle that RNAi therapeutics can be used to target leukemia cells and promise novel treatment options for leukemia patients.

39. Transposon-modified antigen-specific T lymphocytes for sustained therapeutic protein delivery in vivo

Richard ONeil

Patients suffering from anemia caused by renal failure can benefit from treatment with erythropoiesis stimulating agents (ESAs). However, increased adverse cardiovascular events like blood clots, stroke, and heart failure are associated with ESA treatment. Our goal is to develop a cell based therapy utilizing Epstein-Barr virus (EBV) antigen specific T-lymphocytes that will facilitate a continuous, long-term delivery of erythropoietin (EPO) at more physiologically appropriate levels. In these studies we demonstrate the utility of antigen-specific T lymphocytes as a regulatable peptide delivery platform for in vivo therapy. The non-viral piggyBac transposon system enables stable genetic modification of both mouse and human antigen-specific T cells. Modification of murine cells with luciferase for in vivo imaging allows us to visualize T cells after adoptive transfer. We observe long-term T cell engraftment, persistence, and transgene expression enabling detection of modified cells up to 300 days after adoptive transfer and vaccination. Vaccine augmented adoptive transfer of antigen-specific T cells which are transposon modified to express EPO facilitates elevation of hematocrit in mice for more than 20 weeks. We also demonstrate normalization of hematocrit in an adenine-induced nephrotoxicity anemia model. We extend our observations to human T cells demonstrating inducible EPO production from Epstein-Barr virus antigen-specific T-lymphocytes. Our results reveal antigen-specific T-lymphocytes to be an effective delivery platform for therapeutic molecules such as EPO in vivo, with important implications for other diseases that require peptide therapy.

40. Analysis of cardiotoxic mechanism(s) associated with tyrosine kinase inhibitor ponatinib

Anand Prakash Singh, Michael S Glennon, Prachi Umbarkar, Manisha Gupte, Cristi L Galindo, Qinkun Zhang, Thomas Force, Jason Becker, Hind Lal

Background

Ponatinib, a potent pan-BCR-ABL tyrosine kinase inhibitor holds significant promise in the treatment of chronic myelogenous leukemia (CML), although the potential cardiotoxicity of this agent remains a concern. In order to overcome ponatinib associated cardiotoxicity, delineation of linked cardiotoxic mechanisms and potential rescue methods are urgently warranted.

Objectives

The objectives of the study are to identify key signaling pathway(s), inhibition of which accounts for the cardiotoxicity associated with ponatinib and potential rescue methods.

Methods

In this study, we employed direct in vivo drug screening in zebrafish for the prediction of cardiotoxicity.

Results

Ponatinib leads to cardiomyocyte apoptosis, elevation in BNP level and decrease in heart rate leading to cardiac dysfunction in Zebrafish. Consistently, in cultured rat cardiomyocytes, ponatinib was found most cytotoxic drug among all the approved CML TKIs. Mechanistically, ponatinib inhibits the essential prosurvival AKT and ERK signaling pathway, resulting to cardiomyocyte apoptosis. Additionally, we evaluated the cardio-protective effects of Neuregulin-1β to limit ponatinib toxicity. Neuregulin-1β treatment significantly protects ponatinib-induced

cardiotoxicity by supplementing the essential cardiomyocyte prosurvival AKT/ERK signaling pathways.

Conclusions

This study will advance our mechanistic understanding of ponatinib-induced cardiotoxicity, accelerate the discovery of cardioprotective strategies to prevent and rescue the ponatinib-induced cardiotoxicity.

41. An Examination of faculty diversity in STEM departments of ACC schools

Victoria Mukuni & Ed Smith

We examined the level of faculty diversity in science and science related departments in universities in the Atlantic Coast Conference (ACC).

A total of 135 departments were evaluated through the websites of each of the 15 ACC schools. Our determination of diversity was based on the total number of visually-evident African Americans/Blacks, Hispanics, and women who are faculty members as shown for each department. These numbers included full-time faculty, tenure- and non-tenure track but did not include retired and or part time faculty. The number of minority faculty who hold positions as head of department was also considered. We used web-based resources to identify and verify ethnicity and race of faculty in each department at each school. Of the 15 member schools, Duke, Miami and North Carolina State were the most diverse with 88, 48, and 7, minority faculty.

Of these, Duke had eight African American/Black, 72 women and eight Hispanic faculty. Miami had two Black, 32 women and 14 Hispanic faculty. North Carolina State had eight African American/Black, 64 women and five Hispanic faculty. Clemson, Virginia and Wake Forest were the least diverse with Clemson having a total of 39, of which 35 were women, three Hispanic, and 1 Black/African American. Virginia had a total of 48, of these three were African American/Black, 44 were women and four were Hispanic. Wake Forest had a total of 39 minority faculty, of these zero were African American/Black, 45 were women and seven were Hispanic. Georgia Tech had the most diverse head of departments with a total of four minority heads out of the nine departments while Clemson was the least diverse with no minority head of department. As a leading athletic conference in the nation, with significant number of minority athletes in revenue sports, there is need for partnerships between athletic and STEM departments to reduce the disparity described here. We speculate that faculty diversity investigated here may be a result of diversity in the academic administration of the 15 schools. Duke, for example, has an African American dean of the College of Science.

42. Hyperactivation of mTORC1 drives acquired resistance to the pan-HER tyrosine kinase inhibitor neratinib in HER2 mutant cancers

Dhivya R. Sudhan, Ariella B. Hanker, Angel Guerrero-Zotano, Luigi Formisano, Yan Guo, Qi Liu, Francesca Avogadri-Connors, Richard E. Cutler, Jr., Alshad S. Lalani, Richard Bryce, Alan Auerbach, Carlos L. Arteaga

Background: Tumor genomic profiling has identified patients with cancers harboring activating *ERBB2* (HER2) mutations that are sensitive to HER2 targeted therapies. In the SUMMIT phase

II ‘basket’ trial, a subset of patients with *ERBB2* mutant cancers have exhibited significant clinical benefit from treatment with the pan-HER irreversible tyrosine kinase inhibitor (TKI) neratinib. However, durable responses to neratinib are few, suggesting mechanisms of de novo and acquired drug resistance. Thus, we sought to identify druggable mechanisms of resistance to neratinib.
Results: We utilized 5637 bladder cancer (with $HER2^{S310F}$) and OVCAR8 ovarian cancer (with $HER2^{G776V}$) cells. Neratinib-resistant 5637 and OVCAR8 cells were cross-resistant to the HER2 TKIs afatinib and lapatinib. Immunoblot analysis of neratinib resistant cells showed effective suppression of HER2, EGFR and HER3 phosphorylation. However, they exhibited a striking increase in S6 kinase activity and S6 phosphorylation compared to drug-sensitive parental cells, which was maintained in the presence of supra-pharmacological levels of neratinib (1 μM). S6 phosphorylation and viability of drug resistant cells was completely ablated by the combination of neratinib and the TORC1 inhibitor everolimus, but not with the PI3Kα inhibitor alpelisib, the pan-PI3K inhibitor buparlisib, or the AKT inhibitor MK-2206, suggesting PI3K- and AKT-independent activation of TORC1. Gene set enrichment analysis (GSEA) of RNA seq data from the drug-resistant cells revealed significant enrichment of mTORC1 and K-Ras pathway components. Consistent with these results, whole exome sequencing revealed activating alterations of the Ras pathway; thereby suggesting potential Ras mediated mTOR activation driving neratinib resistance.
Conclusions: These data suggest that hyperactivation of TORC1 promotes acquired resistance to neratinib across histologically distinct *ERBB2*-mutant cancers.

---

43. Shaping the study: An exploratory analysis using intersectionality to guide future research on STEM postdoctoral experiences

Patricia M. Buenrostro, Dara Naphan-Kingery, Oluchi Nwosu-Randolph, Monica L. Ridgeway

The purpose of this exploratory study is to draw on preexisting data and literature to design a new study which focuses on examining how STEM post-doctoral researchers’ in training may have varying experiences based on their intersectional identities (e.g. race and gender). Through a secondary analysis of interview and survey data collected by the EDEFI research team at Vanderbilt University, we conducted an in-depth discourse analysis of 3 interview transcripts of African American post-doctoral researchers within STEM for the purpose of identifying salient themes that would add to current understandings about postdocs. From this work we have generated an interview protocol that was informed by the interviews and literature that aim to draw out individual’s experiences with respect to racism, sexism, ableism, and other forms of discrimination. Preliminary findings indicate that, for these scholars of color, having a personal (non-institutional) support system and drawing on various forms of resilience helped them navigate academic and professional spaces. We believe that our positioning as postdoctoral researchers from various disciplines allows for an interdisciplinary approach to researching postdocs, an understudied experience within the academy.

44. Deficits in apical sodium and water transporters along with maintenance of CFTR account for diarrheal pathology in MYO5B KO mice and patients with MVID

Amy C. Engevik, Melinda A. Engevik, Anne R. Meyer, Mitchell Shub, Hermann Koepsell, Nadia Ameen, Matthew Tyska, James R. Goldenring

Background: Microvillus Inclusion Disease (MVID) is a rare form of congenital diarrhea resulting from inactivating mutations in Myosin Vb (MYO5B). The underlying cause of MVID associated diarrhea is currently unknown. We hypothesize that loss of MYO5B results in aberrant expression of key apical enterocyte membrane transporters that promote the absorption of water. **Methods:** Duodenal tissue was collected for analysis and to generate enteroids from neonatal (3-5 day old) MYO5B KO mice and wildtype littermates (control). **Results**: Immunostaining for phosphorylated ezrin (P-ezrin) in neonatal control mice showed robust expression in the brush border. In contrast, MYO5B KO mice had numerous P-ezrin positive inclusions beneath the brush border. Control mice showed apical localization of NHE3, SGLT1, AQP7 and CFTR. Compared to WT, MYO5B KO mice showed decreased apical expression and increased subapical expression of NHE3, SGLT1 and AQP7. MYO5B KO mice had CFTR positive inclusions, however CFTR was still present on the apical membrane of enterocytes. Consistent with these findings, MVID patient biopsies showed decreased apical expression of NHE3 and SGLT1, but CFTR remained on the apical membrane. Enteroids derived from control and MYO5B KO mice showed proper apical expression of CFTR. A forskolin swelling assay demonstrated that CFTR was functional in MYO5B KO and control derived enteroids. **Conclusions:** Collectively, these data suggest that decreased apical expression of NHE3, SGLT1 and AQP7 may be responsible for the dysfunction in water absorption in individuals with MVID. Furthermore, CFTR may be exacerbating the water loss by secreting chloride into the intestinal luminal, resulting in even further dehydration.

45. Two dimensional materials for Infrared Nanophotonics

Thomas G. Folland, Joseph Matson, Ryan Nolen and Joshua D. Caldwell

Spectroscopy and imaging in the infrared spectral region (between 1 and 100μm in wavelength) can provide invaluable structural and chemical information without significant atmospheric scattering. However, optical components conventionally used at these wavelengths have significant drawbacks – whether it is poor mechanical properties or sensitivity to the environment - and are diffraction limited. Solving these challenges requires both new materials and approaches to optical component design. Two dimensional (2D) crystals are a relatively new class of materials which have a layered structure, giving them unusual properties due to their extreme anisotropy. Here we will show that polaritons in 2D materials can be used for designing infrared optics which beat the diffraction limit. Polaritons consist of a photon coupled with charge in a material (either electrons or polar optic phonons), and behave differently to normal electromagnetic waves. Instead of propagating through free space they propagate along a surface, with an effective 'wavelength' below that of that of normal light. Here, using a combination of simulation and spectroscopic techniques, we show how various infrared optical components can be designed, fabricated and realized using facilities available at Vanderbilt. Specifically, we study infrared filters, waveplates and emitters made from the 2D crystal hexagonal boron nitride, using a combination of attenuated total reflection, infrared microscopy,

and infrared thermal emission measurements. Results indicate that a complete, sub-diffraction spectroscopy systems could be realized using two dimensional materials.

46. From Reef Fish to Climate Change: Using Real Scientific Datasets in K12 Math and Science Classrooms

Matt Wilkins

Despite decades-long efforts to improve STEM capacity and engagement among K12 students, the US still routinely underperforms on international assessments, compared to peer countries. It is now widely recognized that the persistence of this issue may partially be explained by schools' imposition of artificial divisions between subject areas and the continued reliance on rote learning of concepts presented in abstract exercises. As such, there are a growing number of regional efforts to encourage the teaching of interdisciplinary lessons that connect concepts across subjects, encourage active critical thinking, communication, and collaboration, while grounding content in real-world-applications. Scientific studies afford virtually limitless and underutilized possibilities for K12 curricula. Each study provides a basic problem and narrative to draw students into integrative problem solving. Importantly, with the burgeoning Open Access Movement, the data for most new studies is available online. Thus, every scientific study represents a potential basis for immersive lessons that allow students to leverage technology to apply abstract math, science, and engineering concepts and follow in the footsteps of researchers to arrive at solutions to real world problems. I here present examples of how to incorporate real scientific data into middle school curriculum in paper-based and online formats, utilizing worksheets, web-based Shiny apps, and interactive multimedia presentations to achieve greater student ownership and mastery of math and science concepts. I believe that facilitating greater collaboration between researchers and educators to create data-centered STEM curricula should become a priority in our efforts to drastically improve the STEM competitiveness of American students.

47. Origins of interface traps in MoS_2-based field-effect transistors

Andrew O'Hara

Field-effect transistors utilizing few-layer MoS_2 as an n-type channel material were fabricated and characterized by collaborators at the University of Central Florida. The devices utilize either h-BN and Al_2O_3 as the gate dielectric layer. Whereas exfoliated h-BN is transferred directly to the MoS_2, growth of Al_2O_3 via atomic layer deposition (ALD) must be preceded by a nucleation seed layer of either oxidized aluminum (AlO_X) or silicon (SiO_X). Measurements of the density of interface traps (D_{it}) show marked differences in the behavior of each of the three types of fabricated devices. While h-BN exhibits close to acceptable values of D_{it}, the aluminum and silicon based ALD seed layers exhibit significantly increased D_{it} and Fermi-level pinning, respectively. In order to gain insight into the source of interface traps, atomistic models of the three relevant interfaces were constructed. Using density functional theory, we investigate the role that near-interface defects in the dielectric layer, dangling bonds, and accidental dopants in the MoS_2 from seed layer sputtering play in creating interfacial electron traps. These calculations are intended to provide guidance in materials selection and improvements to device processing during fabrication.

48. The sweet spot: How to get middle schoolers to talk about math

Patricia Buenrostro

This research study looks at two middle-school teachers' attention to student thinking through the use of video-based formative feedback (VFF), a process in which teachers' classroom instruction is video-taped and thereafter (within a day or two) used to engage teachers in reflection of their instruction. As part of their involvement in a 5-year mathematics professional development program, both teachers agreed to be a part of the focal study that seeks to understand the ways video can support mathematics teachers in their implementation of ambitious instructional goals. Drawing on video data of coaches and teachers discussing teacher-student interactions (with video-taped classroom as artifact), the author uses ethnomethodology to investigate ways in which video-based coaching afforded and constrained teachers' opportunities to reflect on their articulation of a persistent and perplexing problem of practice: how to facilitate student articulation of their thinking. Preliminary findings reveal that while video afforded opportunities for focal teachers (and coaches) to hone in on student thinking, teachers' and coaches struggled to transition the focus from teacher moves to student thinking. The implications of this study can help inform content-focused mathematics coaching on strategies to help teachers facilitate student discourse. Moreover, the findings illuminate the ways in which video-based reflection can support teachers' sense-making about the complexity of transitioning from direct instruction to facilitation of student thinking.

49. Electron beam-induced synthesis of hexagonal 1H-MoSe2 from square β-FeSe decorated with Mo adatoms

John A. Brehm

50. The Leadership Alliance: Training, Mentoring, and Inspiring

Brittany Allison

The Leadership Alliance, a national consortium of more than 30 leading research and teaching colleges/universities, is united by a shared vision to train, mentor, and inspire a diverse group of students from a wide range of cultural and academic backgrounds into competitive graduate training programs and professional research-based careers. Through one of the Leadership Alliance grants, an Administrative Postdoctoral position was created in The Graduate School, within the Vanderbilt University - Enhancing Diversity in Graduate Education (VU-EDGE) Office. This postdoc would be the Program Coordinator for SYnergistic Network to Enhance Research that Grows Innovation (SyNERGI), and also take an active role in coordinating the Leadership Alliance summer programs, Summer Research Early Identification Program (SR-EIP) and First Year Research Experience (FYRE). These programs increase the readiness and competitiveness of program participants through skill development, professional development, and mentoring. The postdoc position prepares the postdoctoral fellow for an administrative career track within academia. In this presentation, I share experiences and progress thus far with coordinating these Leadership Alliance programs.

51. Two-dimensional PdSe2-Pd2Se3 junctions can serve as nanowires

Sebastian Zuluaga

While the exfoliation of almost all layered materials results in a monolayer with the same atomic geometry as its bulk counterpart, the exfoliation of $PdSe_2$ results in a monolayer with a different atomic geometry and a new stoichiometry, Pd_2Se_3, which is a fusion of two $PdSe_2$ monolayers mediated by Se emission. Here we first report first-principles calculations of lateral junctions between a $PdSe_2$ bilayer and a Pd_2Se_3 monolayer. We find that, while several distinct junction geometries are possible, they all exhibit empty interface states below the conduction band. As a result, light n-type doping of either or both sides, e.g., by halogen atoms replacing Se atoms, leads to a remotely-doped interface, i.e., a one-dimensional conducting nanowire that runs along the junction, in between the two semiconductors. We have fabricated such junctions inside a scanning transmission electron microscope (STEM), but doping and transport measurements are not currently practical.

52. Thermogelling, ABC Triblock Copolymer Platform for Resorbable Hydrogels with Tunable, Degradation-Mediated Drug Release

Mukesh K. Gupta, John R. Martin, Bryan R. Dollinger, Madison E. Hattaway, and Craig L. Duvall

Clinical translation of injectable, polymeric hydrogels as drug delivery depots is significantly hindered by these materials' poor *in vivo* degradability and uncontrolled drug release kinetics. To overcome these challenges, a family of thermoresponsive hydrogels fabricated from selfassembling linear ABC triblock copolymers have been developed and engineered to degrade through either hydrolytic/enzymatic or oxidative mechanisms to control *in vivo* drug release kinetics from polymer hydrogels. In this work, we engineered three triblock copolymers with different 'A' blocks, including ROS-degradable poly(propylene sulfide), slow hydrolytically/enzymatically degradable poly(ε-caprolactone), and fast hydrolytically/enzymatically degradable poly(D,L-lactide-*co*-glycolide); for all three polymers, the 'B' block was comprised of hydrophilic poly(N,N-dimethylacrylamide) while the 'C' block was made of thermally-responsive poly(N-isopropylacrylamide), forming PDN, CDN, and LGDN triblock copolymer formulations, respectively. When dissolved in aqueous solution (5 wt%), these copolymers formed stable micelles at ambient temperature but solidified upon heating to form stable gels at 37 °C. PDN hydrogels were selectively degraded under oxidative conditions as assessed by rheology, whereas CDN and LGDN hydrogels showed differential rates of hydrolytic degradation and were also susceptible to enzymatic decomposition. All three hydrogel formulations elicited minimal cytotoxicity when incubated with human mesenchymal stem cells and hosted robust cellular infiltration *in vivo* when injected subcutaneously in mice. Moreover, polymer solutions loaded with the model drug Nile red demonstrated differential sustained release kinetics *in vivo*, with the drug release rates corresponding with the *in vivo* degradation profiles seen in subcutaneously implanted fluorescently-labeled hydrogels. These collective data highlight the potential use of injectable, thermoresponsive hydrogels with diverse degradation kinetics in cell and drug delivery applications.

53. Intrinsic interfacial van der Waals monolayers: Effect on the superconductivity of monolayer FeSe / SrTiO3

Hunter Sims

It was recently demonstrated that monolayer FeSe on a $SrTiO_3$ (STO) substrate is a superconductor with Tc between 60 and 100 K, compared to 8 K in bulk FeSe. Recent experiments have also revealed that an additional layer of titanium oxide lies between the STO substrate and the FeSe monolayer, but the detailed structure of this interface has remained elusive. Here we use a combination of quantum mechanical calculations and scanning transmission electron microscopy to definitively determine the atomic structure of the monolayer. We find that this monolayer is bonded to both the FeSe film and the substrate by van der Waals interactions and is capable of doping the film in a way that agrees with ARPES measurements and is thought to be favorable for superconductivity. Finally, we note that a similar interface exists between an epitaxial monoclinic VO_2 film grown on a STO substate, which suggests that such van der Waals bonded monolayers may be present at other complex-oxide interfaces.

54. Retracted

55. Theoretical phonon spectroscopy using predictive atomistic simulations

Tianli Feng

Thermal conductivity prediction methods are important for understanding and discovering novel materials with desired thermal performance, for example, high thermal conductivity is desirable for thermal management and low thermal conductivity is required for thermoelectrics. Thermal transport in semiconductors and dielectrics is dominated by atomic (lattice) vibrations. Analogous to photon spectroscopes, which decompose light into different frequencies (colors), phonon spectroscopes can decompose atomic vibrations into different frequencies (modes). Knowledge of mode-wise phonon properties is crucial to identifying dominant phonon modes for thermal transport and to designing effective phononic structures or phonon barriers for thermal transport control. In this talk, two atomic-level simulation methods, i.e., first-principles perturbation theory and molecular dynamics, are advanced to be phonon spectroscopes to address the fundamental as well as emerging questions of thermal transport in a broad range of materials, and to manipulate the thermal transport in nanomaterials by nanoengineering.

56. Single Quantum Dot Tracking and Superresolution Imaging of Plasma Membrane Organization of the Dopamine Transporter

Oleg Kovtun, Ian D. Tomlinson, and Sandra J. Rosenthal

The human dopamine transporter (hDAT) mediates rapid reuptake of synaptic dopamine and thus exerts tight control over the spatiotemporal dynamics of dopaminergic neurotransmission. hDAT membrane nanodomain sequestration and endocytic trafficking recently emerged as two regulatory mechanisms critically important for proper hDAT-mediated dopamine reuptake. We have previously reported the synthesis of a biotinylated cocaine analog IDT444 that permits specific detection of membrane-localized hDAT molecules and enables single particle tracking of hDATs with streptavidin-conjugated quantum dots (Qdots). Here, we show that IDT444 preferentially targets hDAT proteins accumulated in the curved membrane regions of the transfected HEK293 and N2A cells. Single particle tracking of Qdot-tagged hDAT proteins revealed heterogeneous diffusivity spanning several orders of diffusion rate magnitude (0.001-0.1 $\mu m^2/s$) that appeared to be dependent on the local membrane morphological landscape. Superresolution structured illumination microscopy (SIM) of the wildtype YFP-HA-hDAT confirmed that the preferential binding of IDT444-Qdots to the curved membrane regions of hDAT-expressing cells is a consequence, not an artefact, of the polarized expression of the wildtype hDAT. SIM imaging of the defective inward-facing hDAT R60A coding variant showed pronounced redistribution of the R60A variant towards the flat membrane region in both HEK293 and N2A cells. Single particle tracking of YFP-HA-hDAT-WT and YFP-HA-hDAT-R60A using either a biotinylated IDT444 or a biotinylated anti-HA antibody fragment revealed that the R60A variant diffused at a significantly greater rate (nearly ~300% of the wildtype protein), pointing to an intriguing link between hDAT diffusivity and global hDAT membrane organization. Current efforts are aimed at deciphering the plasma membrane organization of endogenous hDAT in dopaminergic neurons derived from a human neural progenitor cell line ReNcell VM.

57. VIR-CLASP reveals unexpected interactions between host-encoded pioneer RNA binding proteins and the pre-replicated RNA genome of Chikungunya virus

Byungil Kim, Sarah Arcos, Katherine Rothamel, Yuqi Bian, Seth Reasoner, and Manuel Ascano

The success of an RNA viral pathogen to infect a cell can be defined by its ability to co-opt host factors, compete for endogenous gene expression machinery, and ultimately copy and re-package its genome using cellular resources and processes. Indeed, a virus that is able to replicate its genome marks a milestone in its lifecycle, having bypassed innate immune systems and is on its way to gathering sufficient viral and host proteins for packaging and assembly. Thus, a particularly vulnerable phase of infection comprises of the steps prior to viral replication. Yet our molecular understanding of host-pathogen interactions, particularly between the viral RNA genome and cellular proteins that would interact with it, are lacking due to an inability to distinguish interactions with first-generation viral genomes versus newly synthesized transcripts. To specifically characterize interactions that occur between pre-replicated viral RNA genomes and cellular proteins, we developed a novel approach termed VIR-CLASP (Virus Induced Ribonucleoside-analog enhanced Cross-Linking And Solid-phase Purification). Using this

approach, we investigated early host-pathogen interactions during infection of human cells with Chikungunya virus (CHIKV) that is re-emerging as a global threat. We report the identification of hundreds of direct interactions between host cellular proteins and pre-replicated CHIKV genome. Of these, we characterize and functionally validate the biological impact of three classes of RNA-binding proteins, and find that they play critical antagonistic or facultative roles during replication. As VIR-CLASP does not rely on sequence-specific isolation of viral nucleic acids, our approach is utilizable to potentially all RNA viruses of interest.

---

58. Dual random lattice modeling of erosion in flood protection infrastructure

Alessandro Fascetti

The future of civil infrastructure is in building intelligent and resilient systems that organically interact (i.e., inform as well as adapt to demands) with local communities and decision makers in order to function efficiently and effectively.

My research vision integrates modeling and simulation, remote sensing and decision making technologies in a rigorous and systematic fashion to develop the next generation of intelligent and resilient civil infrastructure systems. My objective is advancing in science and technology in infrastructure protection and resilience with the twofold objective of mitigating the effects of extreme events on the population, as well as improving day-to-day operations and maintenance of the infrastructure.

The focus of my research is on intelligent and data-driven, cyber-physical infrastructure systems that can safely, efficiently and cost-effectively operate in normal and emergency conditions, and communicate with all stakeholders (i.e., in the private and public sector at local, state, regional, and national levels) to increase infrastructure resilience to natural disasters.

Much of my research integrates state-of-the-art random lattice modeling of the infrastructure and field data obtained by means of Unmanned Aerial Vehicles (UAVs). Figure 1 shows an overview of the research I developed on Flood Protection Systems (FPS). In view of the massive size of these systems, I am employing multiscale simulation and machine learning algorithms to efficiently monitor and predict the response of the infrastructure throughout the service life. Machine learning models are also used to mitigate the error propagation due to the high level of uncertainties that FPS modeling naturally exhibits.

Tightly integrated with the physical modeling and simulation tools, I am developing novel remote sensing approaches specifically designed for infrastructure systems. Geolocalized information generated by remote sensing will allow detailed tracking of the structural state, deformation and damage accumulation over time. Different types of sensors that are being investigated include: (1) LiDAR sensors, which allow accurate characterization of 3-dimensional objects by scanning them with laser beams; and (2) Multispectral cameras, which are imaging systems that capture image data within specific wavelength ranges across the electromagnetic spectrum and allow for the 3-dimensional reconstruction of objects by photogrammetry.

59. Osteopontin provides a survival signal for intestinal intraepithelial lymphocytes in mice

Ali Nazmi, Danyvid Olivares-Villagomez, and M. Blanca Piazuelo

Intraepithelial lymphocytes (IEL) are a diverse immune population residing in between intestinal epithelial cells, which possess important roles during mucosal immune responses. The IEL family comprises cells such as TCRαb$^+$CD4$^+$, TCRαb$^+$CD8$^+$, TCRgd$^+$, TCRab$^+$CD8aa$^+$, iCD8a and iCD3$^+$, among others. Osteopontin (OPN), a pleiotropic cytokine encoded by the Spp-1 gene, is well known for its function in tissue remodeling, modulation of Th1 responses development, maintenance of Th17 function, and homeostasis of NK cells. Herein, we investigated the impact of OPN in the IEL compartment.

We compared the cell numbers of IEL, lamina propria (LP) lymphocytes and splenocytes from Spp-1$^{-/-}$ and wildtype (WT) mice. OPN deficiency reduced the number of TCRγδ$^+$, TCRβ$^+$CD4$^+$, TCRβ$^+$CD8α$^+$ and TCRβ$^+$CD4$^+$CD8α$^+$ IEL, but had no effect on LP and spleen lymphocytes. In *in vitro* studies, IEL from WT mice cultured in the presence of rOPN showed better survival rates than IEL incubated alone. The increased survival was blunted to control levels when CD44, a receptor for OPN, was blocked with anti-CD44 antibody. When total T cells (including T_{regs}) from WT splenocytes were transferred into Spp-1$^{-/-}$Rag-2$^{-/-}$ and Rag2$^{-/-}$ mice, we observed that although OPN deficiency did not affect donor-derived IEL reconstitution at day 7 post-transfer, it decreased the number of CD4$^+$ and CD4$^+$CD8α$^+$ IEL at day 28 post-transfer. As expected, Rag-2$^{-/-}$ mice remained healthy throught the experiment; however, Spp-1$^{-/-}$Rag-2$^{-/-}$ recipient mice presented a remarkably loss of body weight and colon inflammation.

Together, our results indicate that OPN is a critical survival signal for IEL via CD44, and that OPN-deficiency promotes development of colitis even in the presence of T_{regs}.

60. Chemically stabilized DT-MoS2 alloys for enhanced electrocatalytic activity

P. Manchanda, Shi-Ze Yang, Y. Y. Zhang, Yongji Gong, Gonglan Ye, Pulickel Ajayan, Matthew F. Chisholm, Wu Zhou, S. T. Pantelides

The hydrogen evolution reaction (HER) refers to the splitting of H_2 molecules to get atomic hydrogen. The best-known HER catalyst is Pt, but scarcity and the high cost of Pt limit its utility in large-scale applications. MoS_2, owing to the abundance of its component elements, low cost, and good stability has emerged as a good alternative to Pt. However, the basal plane of the 2H phase of MoS_2 is catalytically inert and only edges catalyze the hydrogen production mechanism. In this work, we use density functional theory calculations and electron microscopy to demonstrate that distorted-T (DT) phase MoS_2 can be stabilized by alloying with 50% rhenium, which leads to significant improvement in HER performance. We find that the DT phase $Re_{0.55}Mo_{0.45}S_2$ shows low overpotential and, therefore, results in enhanced electrocatalytic activity. In order to evaluate HER activity and the mechanism responsible for low overpotential in Re-doped MoS_2 monolayers, we calculated the Gibbs free energy (ΔG_H) for hydrogen adsorption. We find that ΔG_H for $Re_{0.55}Mo_{0.45}S_2$ strongly depends on the local environment and the most active sites are S atoms surrounded by three Mo atoms, with ΔG_H being close to zero.

61. NFPws: A web server for delineating eptiope-specific broadly neutralizing antibody responses from serum neutralization data

Nagarajan Raju, Ivelin Georgiev

A better understanding of antibody responses to HIV-1 infection in humans can provide novel insights for the development of an effective HIV-1 vaccine. Neutralization fingerprinting (NFP) is an efficient and accurate algorithm for delineating the epitope specificities found in polyclonal antibody responses to HIV-1 infection[1-2]. Here, we report the development of NFPws, a webserver implementation of the NFP algorithm. The server takes as input serum neutralization data for a set of diverse viral strains as input, and uses a mathematical model to identify similarities between the serum neutralization pattern and the patterns for known broadly neutralizing monoclonal antibodies (bNAbs), in order to predict the prevalence of bNAb epitope specificities in the given serum. In addition, NFPws also computes and displays a number of prediction quality estimators, including a normalized residues score, a median delineation score and a frequency of random signals. For a given serum, these values can be used to estimate the confidence in the predicted antibody specificities, as well as the likelihood of presence of novel, previously uncharacterized, antibody specificities. Overall, the NFPws server will be an important tool for the identification and analysis of epitope specificities of broadly neutralizing antibodies responses against HIV-1.

References

1. Doria-Rose et al. (2017) Mapping Polyclonal HIV-1 Antibody Responses via Next-Generation Neutralization Fingerprinting. PLoS Pathog 13(1): e1006148
2. Georgiev IS et al. Delineating antibody recognition in polyclonal sera from patterns of HIV-1 isolate neutralization. Science.

62. Interface-induced emergent properties in self-assembled La1-xSrxMnO3/La1-ySryMnO3 heterostructures

Summayya Kouser, Saurabh Ghosh, Mohammad Saghayezhian, Hangwen Guo, Ward Plummer & Sokrates Pantelides

The strong correlation of charge, lattice, spin and orbital degrees of freedom in manganites provides a rich phase diagram for $La_{1-x}Sr_xMnO_3$ (LSMO) that ranges from canted antiferromagnetism (AFM) to ferromagnetism (FM) to paramagnetism (PM). Here we report the growth of self-assembled ($La_{0.67}Sr_{0.33}MnO_3/La_{0.73}Sr_{0.27}MnO_3/SrTiO_3$) thin-film heterostructures that show unusual magnetic properties like exchange bias, spontaneous magnetic reversal and inverted hysteresis, with substantial suppression of octahedral tilts in La-poor region. Using first-principles calculations, we provide a theoretical understanding of the correlation of structural and magnetic properties observed in these self-assembled heterostructures and complement the experiments. We address the following three questions: (I) How does change of x in $La_{1-x}Sr_xMnO_3$ affect magnetism? (II) What is the origin of the observed exchange bias? and (III) How do we explain the suppression of octahedral tilts in $La_{0.67}Sr_{0.33}MnO_3$ identified as critical for the novel magnetic properties?

Acknowledgements: This work is supported by DOE grant numbers **DE-FG02-09ER46554** and **DE-SC0002136.**

63. Dietary zinc restriction compromises host immunity to Acinetobacter baumannii lung infection

Lauren D. Palmer, Lillian J. Juttukonda, Kelli L. Boyd, Eric P. Skaar

Zinc deficiency affects one third of the global population, and the World Health Organization estimated that zinc deficiency contributes to up to 16% of lower respiratory infections globally. However, the molecular mechanisms linking zinc deficiency and pneumonia remain uncharacterized. In the United States, intensive care unit patients are at increased risk for zinc deficiency and infection by the opportunistic pathogen *Acinetobacter baumannii*. Because zinc acquisition is critical to *A. baumannii* during lung infection, we established a murine model of zinc deficiency and *A. baumannii* pneumonia. In this model, zinc deficient mice suffer significantly higher mortality within 24 h of infection, establishing a system to probe host and bacterial response to dietary zinc restriction. At 24 h post infection, zinc deficient mice have higher bacterial burdens, higher production of pro-inflammatory cytokines, lower production of anti-inflammatory cytokines, and higher rates of inflammation and immune cell apoptosis. In order to understand how dietary zinc alters the host environment, *A. baumannii* genes important for survival in zinc deficient mice were identified using transposon sequencing (Tn-seq). This analysis identified key *A. baumannii* metabolic pathways as important during infection of the zinc deficient host including metal acquisition. Further experimentation revealed that zinc deficient mice have a defect in nutritional immunity, the innate immune response that restricts pathogen access to nutrient metals. Together, these results indicate that dietary zinc restriction causes host immune dysregulation and failure to control bacterial replication, which demand additional metabolic requirements of the bacterial pathogen.

64. Comparison of RSV hospitalized children with and without underlying medical condition

Einas Batarseh

Introduction

The majority of hospitalized children with Respiratory Syncytial Virus (RSV) do not have underlying medical conditions (UMCs). Therefore, we sought to compare clinical characteristics and outcomes of RSV-positive hospitalized children with the presence and absence of UMCs.

Summary

- We conducted a prospective year-round viral surveillance study comparing children <2 years hospitalized with respiratory symptoms and/or fever.
- We compared children with RSV infection in the presence and the absence of UMC.
- Results showed significant differences in age, chest radiographs, admission diagnosis, the use of antibiotics during hospitalization, death, and vitamin-D levels between the two groups.

Further investigations using multivariable analysis will be important to target RSV preventative measures.

65. Bactericidal Mechanisms of Arachidonic Acid against Staphylococcus aureus

William Beavers

Staphylococcus aureus is a pathogen capable of infecting nearly every organ in the vertebrate host. The pervasiveness of this pathogen and the widespread overuse of antibiotics have heralded the emergence of antimicrobial resistant strains, including methicillin resistant *S. aureus* (MRSA). This presents the desperate need to identify and validate targets for the development of new therapies. Arachidonic acid (AA) is a polyunsaturated fatty acid produced by humans, but not by bacteria. In response to bacterial infections, AA serves as a precursor to both pro- and anti-inflammatory bioactive lipid metabolites. Additionally, AA is bactericidal to *S. aureus* independent of its role in signaling. We discovered that AA is bactericidal to *S. aureus* through a lipid peroxidation mechanism, where AA is oxidized to isolevuglandin (IsoLG). IsoLGs elicit toxicity in eukaryotic cells by reacting irreversibly with the ε-amine of lysine, often compromising protein function; however, this mechanism has not been defined in bacteria. AA toxicity is alleviated in *S. aureus* with the administration of antioxidants as well as IsoLG specific scavengers. Further, this toxicity is exacerbated through the increased generation of reactive oxygen species. To further understand the mechanisms by which *S. aureus* avoids AA toxicity, we selected for resistant mutants. Whole genome sequencing identified a non-sense mutation in LytR-Cpsa-Psr A (*lcpA*); and deletion of *lcpA* confers *S. aureus* with resistance to AA toxicity. LcpA ligates wall teichoic acids (WTA) to the cell wall, indicating that WTA may sensitize *S. aureus* to AA toxicity. However, blocking the synthesis of WTA through *tarO* deletion or inhibition sensitizes *S. aureus* to AA toxicity, indicating a more nuanced role for Δ*lcpA* and WTA in resisting polyunsaturated fatty acid stress. Future experiments will define the molecular mechanisms by which *Δlcp*A alleviates AA toxicity in *S. aureus*.

66. Acute Gastroenteritis Illness Severity by Pathogen and Rotavirus Vaccine Status

Lubna Hamdan, MD, Bhinnata Piya, MPH, Laura S Stewart, PhD, Einas Batarseh, MD, Christopher J Fonnesbeck, PhD, John R Dunn, DVM, PhD, Aron J Hall, DVM, MSPH, Daniel C. Payne, PhD, MPH, Natasha Halasa, MD, MPH

Background:
Viral pathogens are the most common cause of acute gastroenteritis (AGE) and can be associated with severe illness.
Objective:
Using Modified Vesikari Score (MVS) parameters, we compared AGE illness severity by viral pathogen and by rotavirus vaccination status in rotavirus positive-children.
Methods:
AGE surveillance for children aged >14 days and <18 years was performed at Vanderbilt Children's Hospital in the inpatient, emergency department (ED), and outpatient (OP) settings. Stool specimens were tested by RT-qPCR for norovirus, sapovirus, and astrovirus; and by ELISA for rotavirus (RoV) VP6 antigen (Rotaclone$^{@}$). We used the MVS parameters and stratified by single virus detection and vaccination status in rotavirus-positive children.
Results:

From 12/2012-11/2015, 3705 AGE cases were enrolled and 2889 (78%) children provided stool specimens. Testing revealed 565(20%), 231(8%), 224(8%), and 89(3%) stools tested positive for only norovirus, sapovirus, rotavirus, and astrovirus, respectively. The median MVS parameters of patients with norovirus (6.8), sapovirus (6.9), or astrovirus (6.9) were all significantly lower ($p<0.05$) than that among rotavirus patients (8.3). Table 1 compares rotavirus-positive children by vaccination status.

Table 1.

	Rotavirus Positive with any rotavirus vaccine dose n=154	Unvaccinated Rotavirus-positive n=70	p-value
Modified Vesikari Score	8 (7-10)†	9 (7-10)†	0.68
Age (Months)	**1.8 (1.2-3.4)**†	**4.4 (1.5-8.2)**†	**<.01**
Diarrhea (duration) days	2 (1-3)†	3 (1-3)†	0.27
Max no. of diarrheal stools/ 24 hour period (in the course of the disease)	6 (4-8)†	5 (4-8)†	0.73
Vomiting duration (day)	2 (1-3)†	2 (1-3)†	0.89
max no. of vomiting episodes/ 24 hour period (in the course of the disease)	5 (3-8)†	5 (3-9)†	0.58
Max recorded fever	102 (101-104)†	102 (101-104)†	0.98
IV Rehydration	**18 (11.7%)**	**23 (32.9%)**	**<.01**
Hospitalization	**13 (8.4%)**	**16 (22.9%)**	**<.01**
Emergency Department/ Hospitalized follow up.	5 (5.3%)	2 (3.6%)	0.65

†All continuous variables in Median (IQR).
*Pearson's $\chi 2$ test for categorical and Wilcoxon rank-sum (Mann-Whitney) test for continuous variables.

Conclusion:

Despite the decline in rotavirus incidence in a post-rotavirus vaccine era, the severity of AGE illness in rotavirus-positive children remains greater than other viral pathogens. Although the AGE severity for rotavirus-positive children was not statistically different by vaccination status, unvaccinated children were older, and more likely to be hospitalized and to require IV hydration. These data highlight the benefits of rotavirus vaccination and support efforts to maximize vaccination coverage.

67. MntE is essential for maintaining intracellular manganese homeostasis in *Staphylococcus aureus*

Caroline M. Grunenwald, Jacob E. Choby, William N. Beavers, Eric P. Skaar

Staphylococcus aureus is a significant cause of human morbidity and mortality. Manganese (Mn) is an essential micronutrient and plays an important role in *S. aureus* physiology; thus acquisition of Mn is critical for pathogenesis. Paradoxically, excess Mn is toxic, therefore maintaining intracellular Mn homeostasis is essential for survival. Here we describe a putative Mn exporter, MntE, which is a member of the Cation Diffusion Facilitator protein family and conserved among other Gram-positive pathogens. Upregulation of *mntE* transcription in response to excess Mn is dependent on the presence of *mntR,* a transcriptional repressor of the *mntABC* Mn uptake system. Inactivation of *mntE* or *mntR* leads to reduced growth in media supplemented with Mn, but not other metals, which is complemented by constitutive expression of *mntE in trans*. This demonstrates MntE is required for resistance to excess Mn and MntE activity is highly specific for Mn. Inactivation of MntE results in intracellular accumulation of Mn, further suggesting that MntE functions as a Mn exporter. Additionally, *mntE* mutants are more sensitive to HOCl and paraquat, indicating Mn homeostasis is critical for resisting oxidative stress. Mutants lacking either *mntR* or both *mntE* and *mntR* show reduced burdens in murine hearts and spleens following systemic infection. Combined, these data support a model where MntR regulates Mn uptake through MntABC and Mn export through MntE and suggests Mn efflux contributes to bacterial survival during infection. Future work will further define MntR regulation of *mntE* and the contribution of Mn homeostasis to *S. aureus* pathogenesis.

68. A Host Immune Protein Guides *Clostridium difficile* Niche Selection in the Gut

Christopher A. Lopez, Joseph P. Zackular, Reece J. Knippel, and Eric P. Skaar

The large intestines house a diverse microbiota that collectively protect against invasion by pathogenic bacteria, termed colonization resistance. *Clostridium difficile*, an anaerobic spore-forming bacterium, takes advantage of antibiotic-induced disruption of colonization resistance to initiate gut colonization. However, subsequent to initial colonization *C. difficile* must establish a niche where the pathogen can compete with the resident microbes for nutrients while resisting host-mediated changes to the nutrient environment. The limiting nutrients governing *C. difficile* interactions with the microbiota and the role of the host in manipulating access to those nutrients during *C. difficile* infections (CDI) are unclear. One arm of the host response during CDI that impacts the gut environment is the release of the protein calprotectin, which binds and sequesters the nutrient metals zinc, manganese, nickel, and iron. In a mouse model of CDI we found that the presence of calprotectin in wild type mice led to an altered microbiota compared to mice lacking functional calprotectin. Additionally, the presence of calprotectin was associated with shifts in *C. difficile* gene expression, particularly in genes required for proline fermentation. We thus hypothesize that proline metabolism is regulated in part through the availability of nutrient metals and that this metabolic shift allows *C. difficile* to grow in the presence of competing microbes. Future work to uncover the role of proline metabolism in the context of infection will provide insight into how the host immune response drives pathogen adaptation to alternate nutritional niches as well highlight strategies used by *C. difficile* to overcome barriers to gut survival.

69. Cerebral blood flow and cerebrovascular reactivity predict cognitive trajectory in older adults

Katie E. Osborn, Dandan Liu, Kimberly R. Pechman, Francis E. Cambronero, Hailey A. Kresge, Samantha R. Herbener, Hanyang Wang, Jaclyn E. Bogner, Jennifer L. Thompson, Sarah L. Lambros, Lily E. Walljasper, Katherine A. Gifford, Timothy J. Hohman, Manus J. Donahue, & Angela L. Jefferson

Cerebral blood flow (CBF) and cerebrovascular reactivity (CVR) changes precede clinical dementia but their associations with memory trajectory are not entirely clear, particularly among carriers of *APOE*-ε4, a molecular modifier of vascular disease and strong genetic risk factor for Alzheimer's disease (AD). Vanderbilt Memory & Aging Project participants free of clinical stroke or dementia (n=282, 73±7 years) underwent T1-weighted magnetic resonance imaging (MRI) to quantify gray matter volume, pseudocontinuous arterial spin labeling MRI for resting CBF (mL/100g/min) and hypercapniainduced CVR, and longitudinal neuropsychological assessment at baseline, 18-month, and 36-months. Linear regressions related baseline regional CBF and CVR to cognitive trajectory across 36 months with comprehensive covariate adjustment for potential confounds. Models were repeated assessing CBF and CVR interactions with *APOE*-ε4 status. Lower CBF across multiple regions predicted steeper memory decline over follow-up (p-values<0.04). There were CBF x *APOE*-ε4 interactions for semantic fluency in which *higher* baseline CBF predicted steeper fluency decline among *APOE*-ε4 carriers only (p-values<0.01). Lower baseline CVR also predicted steeper memory decline across multiple regions (p-values<0.04), with *higher* left temporal lobe CVR predicting steeper decline in delayed recall (0.04). Lower CBF and CVR predicted steeper memory decline. However, higher CBF and CVR among *APOE*-ε4 carriers may reflect hemodynamic compensatory responses to early neurodegenerative changes, predicting worse cognitive prognosis. Consistent with prior research, semantic fluency emerged as a particularly robust early cognitive marker of decline, but its associations appeared limited to *APOE*-ε4 carriers. Pathological hyperperfusion may underlie early semantic fluency and memory impairments among individuals at risk for AD.
Funding: IIRG-08-88733, R01-AG034962, R01-AG056534, R01-NS100980, K24-AG046373, F32-AG058395, T32-MH064913, R25-GM062459, UL1-TR000445, S10-OD023680

70. A metal-responsive transcriptional regulator protects *Acinetobacter baumannii* from manganese limitation and oxidative stress

Erin Green, Lillian J. Juttukonda, Eric P. Skaar

Acinetobacter baumannii commonly infects critically ill patients in hospitals and has become an important global health threat due to its acquisition of multi-drug resistance. Neutrophils inhibit growth of *A. baumannii* through a variety of mechanisms, including the production of ROS and the release of calprotectin, an immune protein that chelates zinc and manganese (Mn). We previously identified a Mn transporter, MumT, which promotes growth of *A. baumannii* during Mn starvation. MumT is encoded adjacent to a LysR-family transcriptional regulator, MumR. Transcription of *mumT* is dependent on MumR, and is heightened in the presence of calprotectin. Because Mn import is a common defense against ROS, we hypothesized that MumT might be important for resisting H_2O_2. Surprisingly, Δ*mumR,* but not *ΔmumT*, was sensitive to H_2O_2, suggesting that MumR regulates other genes that promote H_2O_2 resistance. To determine whether MumR acts through the canonical redox-sensitive regulator OxyR, a Δ*mumR*Δ*oxyR*

mutant was constructed. This mutant was more sensitive to H_2O_2 than Δ*mumR* or Δ*oxyR*, indicating that both proteins activate distinct regulons to promote H_2O_2 resistance. RNA-sequencing was performed to define the regulon of MumR, which revealed a role for MumR in regulating several catabolic pathways. Finally, Δ*mumR* exhibited reduced fitness in a murine model of pneumonia that was restored in neutropenic mice. In summary, these results suggest that MumR resists neutrophil killing by activating a transcriptional program critical for surviving Mn starvation and ROS. Future directions will be aimed at further characterizing the functions of genes in the MumR regulon under these conditions.

71. Differential effects of angiotensin II type I receptor blockers on reducing TGFβ signaling and intraocular pressure in the mouse retina

Ralph Hazlewood

Transforming growth factor beta (TGFβ) is believed to play an important role in glaucoma pathogenesis. Angiotensin II type 1 receptor blockers (ARBs), commonly used to treat systemic hypertension, attenuate TGFβ signaling, and exhibit neuroprotection in glaucoma models, but their ability to lower IOP is debated. Currently, there are eight ARBs in clinical use each with different chemical structures and modes of binding to angiotensin II type 1 receptor. The purpose of this study is to investigate ARBs as potential treatments for glaucoma.
Losartan, irbesartan, telmisartan, or vehicle controls were administered orally in the chow to normal 3 month-old male, C57BL/6 mice for 7 days. Before and after treatment, IOP was measured by TonoLab and blood pressure (BP) by tail-cuff method. Following measurements, mice were sacrificed and eyes evaluated for TGFβ signaling by immunohistochemistry.
BP was significantly reduced in all ARB treatment groups. IOP was not affected by losartan administration at time-points tested. However, IOP was significantly reduced after 3 days and 7 days of treatment with irbesartan ($p < 0.05$) and after 7 days treatment with telmisartan ($p < 0.05$). In the retina, telmisartan treatment also caused significant reductions in TGFβ signaling assessed by phosphorylated SMAD2+ cell count and protein expression ($p < 0.05$).
Oral administration of all ARBs tested results in lower systemic BP and reduced TGFβ signaling in the eye. IOP-lowering capability varies by specific ARB used, with losartan having no effect. Conversely, telmisartan and irbesartan administration results in significant lowering of IOP, while telmisartan also reduced TGFβ signaling in neural retina. Considering significant roles of BP, IOP and TGFβ regulation in glaucoma development/progression, telmisartan may offer the most promising treatment to glaucoma.

72. Histamine at the host-pathogen interface during *Acinetobacter baumannii* infection

Jessica Sheldon and Eric P. Skaar

Acinetobacter baumannii is an emerging pathogen that poses a global health threat due to a lack of viable therapeutic options. The success of *A. baumannii* is thought to be partly due to its ability to successfully compete with the host for essential nutrients. As a facet of innate immunity, the host restricts the availability of essential metals to curtail bacterial proliferation. To counter this restriction, bacteria possess numerous mechanisms to obtain these metals, including through the production of small secreted siderophores, which bind and deliver iron to the bacterium. *A. baumannii* elaborates up to ten structurally distinct siderophores; acinetobactin

and pre-acinetobactin, baumanoferrins A and B, and fimsbactins A-F. Here we demonstrate that *A. baumannii* synthesizes histamine, a key precursor molecule to the production of acinetobactin, through the activity of a putative iron-regulated histidine decarboxylase, *basG*. While functional redundancy by the other siderophores largely masks the role of *basG in vitro*, we demonstrate that *basG* influences survival of *A. baumannii in vivo*. Further, we show that histamine detection is increased in mice infected with wild-type *A. baumannii* versus those mock-infected or infected with a *basG*-deficient strain. Using nanoString technology, we reveal host histidine decarboxylase (hHDC) expression is also upregulated in *A. baumannii* infected hosts, suggesting it may also contribute to the presence of histamine at the host-pathogen interface. Given that histamine is an important immunomodulator, these results suggest that histamine production may play an important role not only in iron acquisition by *A. baumannii*, but in the overall pathophysiology of infection.

73. Heterogeneity in Schizophrenia: Parsing by Temperament

Brandee Feola, Kristan Armstrong, Stephan Heckers, & Jennifer Urbano Blackford

Background: Schizophrenia is a complex disorder with heterogeneous presentations. One possible source of heterogeneity is individual differences in temperament. Early differences in temperament are associated with increased prevalence of multiple psychiatric disorders. More specifically, inhibited temperament is a major risk factor for developing anxiety disorders. The current study examined the rate of inhibited temperament and schizophrenia and characterized the patients with inhibited temperament in terms of anxiety, psychosis, and functional outcomes.
Methods: Participants were patients with schizophrenia (N = 174, 66.0% male) and healthy controls (N = 186, 58.6% male). Temperament was assessed by a validated self-report measure (Retrospective Self Report of Inhibition). Participants were classified as having inhibited, average, or uninhibited temperament based on 15^{th}/85^{th} percentiles from normative data. The following data were also collected: anxiety diagnosis, anxiety symptoms, psychosis symptoms, and quality of life. Analysis of Variance were used to test for group differences in the continuous measures and chi-square analyses tested for group differences in the categorical variables.
Results: 32.8% of patients with schizophrenia had an inhibited temperament compared to 5.4% of healthy controls ($p < 0.01$). Within patients with schizophrenia, temperament predicted higher likelihood of anxiety diagnosis, higher levels of anxiety symptoms, and lower quality of life ($p < 0.01$ for all findings; η_P^2 ranged from 0.07-0.24).
Conclusions: The current study parsed the heterogeneity of patients with schizophrenia using temperament to explain variation in anxiety symptoms and functional outcomes. These results suggest a novel neurodevelopmental pathway to schizophrenia characterized by temperament.

74. Inhibition of CDK4/6 and Pi3Kγ modulates mammary tumor immune microenvironment to enhance response to immunotherapy

Stacey Mont

An anti-tumor immune response is critical in achieving immunotherapy driven tumor regression. Despite clinical advances in immunotherapies, patients with breast cancer have been only moderately responsive. In this study, we tested whether inhibition of CDK4/6 and Pi3Kγ inhibition can augment the immunotherapy response. Our results show that in breast cancer models, palbociclib (CDK4/6i) in combination with anti-CD137, can inhibit tumor growth. We also assessed

the effect of palbociclib in a post-surgical model, where treatment began 5 days after injecting 37,000 MMTV-PyMT breast cancer cells. In this model, a significant inhibition of tumor growth was reported with palbocliclib. Additionally, we demonstrate that palbociclib can be quite effective in total tumor burden in the PyMT-FVB spontaneous breast cancer model. Furthermore, mice treated with palbociclib in this model had an increase in CD3+ cell infiltrate in tumor lung metastasis. We used the Pi3Kɣ-null mice treated +/- palbociclib to assess the dual inhibition of CDK4/6 and Pi3Kɣ on MMTV-PyMT tumors. Here, we demonstrate an increase in CD45+ cells within the tumor microenvironment and an increase in MHC class II+, antigen-presenting macrophages upon palbociclib treatment. Additionally, gene expression analysis of chemokines in palbociclib treated MCF-7 cells induced the expression of CCL4, CCL5, CXCL9, CXCL10, and CXCL11, each of which are implicated in T-cell tumor-homing. Overall, our findings suggest that CDK4/6 inhibition and dual inhibition targeting Pi3Kɣ may enhance tumor immunogenicity. Dual inhibition of CDK4/6 and Pi3Kɣ is of high clinical relevance and may be used in combination with immunotherapies in the treatment for breast cancer.

75. Fluency in symbolic arithmetic refines the approximate number system in parietal cortex

Macarena Suarez Pellicioni

The objective of this study was to investigate, using a brain measure of ANS acuity, whether the precision of the ANS is crucial for the development of symbolic numerical abilities (i.e. *scaffolding hypothesis*) and/or whether the experience with symbolic number processing refines the ANS (i.e. *refinement hypothesis*). To this aim, 38 children solved a dot comparison task inside the scanner when they were approximately 10 years old (Time 1) and once again approximately 2 years later (Time 2). To study the *scaffolding hypothesis,* a regression analysis was carried out by entering ANS acuity at T1 as the predictor and symbolic math performance at T2 as the dependent measure. Symbolic math performance, visuospatial WM and full IQ (all at T1) were entered as covariates of no interest. In order to study the *refinement hypothesis*, the regression analysis included symbolic math performance at T1 as the predictor and ANS acuity at T2 as the dependent measure, while ANS acuity, visuospatial WM and full IQ (all at T1) were entered as covariates of no interest. Our results supported the *refinement hypothesis*, by finding that the higher the initial level of symbolic math performance, the greater the IPS activation was at T2 (i.e. more precise representation of quantity). To the best of our knowledge, our finding constitutes the first evidence showing that expertise in the manipulation of symbols, which is a cultural invention, has the power to refine the neural representation of quantity in the evolutionarily ancient, approximate system of quantity representation.

76. Methylation of CA repeats as a regulator of memory formation

Celeste Greer

Methylation of the cytosine nucleotides of DNA is a potent regulator of memory formation. While many differentially methylated regions have been identified that correlate with memory formation, little is known about how methylation of specific sites or motifs affects gene expression. Through data-mining of a previously published methyl-DNA immunopreciptiation sequencing (MeDIP-seq) experiment from mice that have acquired a new memory, I found that many regions with long repeats of the base pairs CA become highly methylated in neurons

during learning. This is a surprising finding because simple repeats in non-coding regions have been considered 'junk DNA.' However, these repeats are found with high frequency in and around many important learning- and memory-associated genes in the mouse and human genome. To look into the function of these repeat domains, we designed a transcription factor that can methylate these simple repeat regions. Increasing simple repeat methylation regulates the expression of several genes important for memory formation. Additionally, genes whose expression is regulated by methyl-CpG binding protein 2 (Mecp2), which is mutated in a pervasive developmental disorder called Rett syndrome, contain more CA-repeats than other genes of similar length. Mecp2 has been shown to bind methylated CA dinucleotides, and this points to a potential mechanism where Mecp2 binding is redirected to methylated CA-repeat regions during memory formation to derepress the transcription of relevant genes. This work shows a potential new function for these previously ignored parts of the genome.

77. Noninvasive characterization of cerebral hemodynamics in sickle cell anemia

Meher Juttukonda

Sickle cell anemia (SCA) is a genetically-inherited disorder that results in the production of erythrocytes with hemoglobin-S, resulting in anemia and elevated risk of vasculopathy, silent cerebral infarction, and stroke. Unlike in children with SCA, no standard exists for stratifying adults with SCA to aggressive therapies, such as blood transfusions, for primary stroke prevention; instead, transfusions are often administered for secondary stroke prevention. Brain tissue oxygen extraction fraction (OEF) and cerebral blood flow (CBF) have been identified as potential markers of impairment in SCA. While PET methods for assessing these markers exist, they are not utilized for longitudinal monitoring due to technical challenges and the need for ionizing radiation. The purpose of this study was to utilize noninvasive magnetic resonance imaging (MRI) to evaluate hemo-metabolic response to transfusion. We utilized noninvasive MRI methods to evaluate how OEF and CBF adjust after transfusion in adults with SCA. Our results showed that OEF reduced on average, while CBF did not change significantly. Furthermore, the OEF reduction paralleled increases in hematocrit but was unrelated to the reduction in hemoglobin-S. These findings imply that most patients receiving transfusions operate near autoregulatory reserve capacity even after transfusion, and improving oxygen delivery by increasing hematocrit can be visualized noninvasively with OEF-MRI.

78. Hippocampal Network Dysfunction and Relational Memory Deficits in Schizophrenia

Suzanne N. Avery, Kristan Armstrong, Baxter P. Rogers, Stephan Heckers

Background: Functional dysconnectivity, or the loss of coherence of functional neural networks, has long been thought to underlie cognitive impairment in schizophrenia. In particular, individual connections with the hippocampus—a consistent focal point of structural and functional changes in schizophrenia—have been associated with the marked memory deficits observed in patients. However, only recent technological advances have enabled the large-scale exploration of functional networks with accuracy and precision. Here, we use graph theory to investigate the relationship between hippocampal functional networks and memory deficits in schizophrenia.

Methods: We examined resting-state connectivity in 45 schizophrenia spectrum disorder patients and 38 healthy controls. Modularity was calculated for a core hippocampal-medial temporal lobe cortex (MTLC) network and an extended hippocampal-cortical network; follow-up analyses tested anterior and posterior divisions. Correlations were examined between modularity and relational memory ability.
Results: Hippocampal-MTLC modularity was lower in schizophrenia patients than controls ($F = 6.14$, $p = .02$), with a similar, though non-significant, pattern found in the hippocampal-cortical network ($p = .22$). Relational memory was also markedly impaired in patients ($X^2 = 30.18$, $p < .0001$). Patients and controls showed a distinct brain-behavior relationship that differed by network and anterior/posterior division—while relational memory in control subjects was associated with lower anterior hippocampal-cortical modularity ($r = -.48$, $p = .004$), relational memory in schizophrenia patients trended with lower posterior hippocampal-MTLC network modularity ($r = -.32$, $p = .07$).
Conclusions: Our findings support a model of abnormal resting-state cortico-hippocampal network coherence in schizophrenia, which may contribute to relational memory deficits.
Keywords: psychosis, resting-state fMRI, functional connectivity, graph theory, modularity

79. Action potential triangulation and instability in TnT-I79N human iPSC-CMs

Lili Wang

Cardiac troponin T (TnT) I79N mutation causes hypertrophic cardiomyopathy. Previous studies showed that I79N mutation increases myofilament Ca sensitivity, which contributes to the development of cardiac arrhythmias. However, the arrhythmia mechanism remains elusive. Here, we studied the effect of I79N mutation on action potential (AP) in human induced pluripotent stem cell-derived cardiomyocytes (hiPSC-CMs). APs were recorded in current clamp mode without any exogenous Ca buffers added to the intracellular solutions. There was no difference in resting membrane potential, peak amplitude and time-to-peak between I79N and control CMs. I79N mutation significantly shortened early repolarization (APD30, APD50 and APD70), whereas late repolarization (APD90) did not change. As a result, APs from I79N CMs exhibited triangulation (APD(90-30)/90: I79N 0.35±0.03 vs. control 0.28±0.01, $P<0.01$) and beat-to-beat instability (Average ratio of interquartile range to median APD50: I79N 0.12±0.02 vs. control 0.07±0.01, $P<0.05$) compared to control. The AP triangulation and instability were reproduced with 3 μM Ca-sensitizing agent EMD in control CMs. Pretreatment with 3 μM Ca-desensitizer blebbistatin or excess cytosolic buffering (by adding 14 mM EGTA to intracellular solution) prevented AP triangulation in I79N CMs. How could the I79N mutation cause AP triangulation in CMs? In ventricular CMs, Ca extrusion via Na-Ca exchanger (NCX) generates inward current that contributes to repolarization. Since the I79N mutation increases myofilament Ca buffering and causes the smaller Ca transients, NCX currents could be reduced and thereby shorten the early repolarization. To test this hypothesis, NCX-mediated Ca extrusion was blocked by replacing extracellular Na^+ with Li^+. NCX block with Li^+ eliminated the AP differences between I79N and control CMs. Taken together, our results indicate that I79N mutation shortens the early repolarization of AP via a NCX-mediated mechanism, resulting in AP triangulation and instability, both of which would increase arrhythmia risk.

80. Response to transdermal nicotine in Late Life Depression alters electrophysiological responses - A pilot study

Alexander C. Conley, Kimberly Albert, Jason Gandelman, Brian D. Boyd, Paul A. Newhouse & Warren D. Taylor

Late Life Depression (LLD) is characterized by poor antidepressant response, as well as poorer cognitive and electrophysiological performance compared to age-matched controls. Based on previous research showing transdermal nicotine improving cognitive outcomes in mild cognitive impairment, we examined whether transdermal nicotine benefits mood and electrophysiological performance in LLD. In this pilot study, 9 patients with LLD (4 male, μ age = 64.9 ± 4.7 years) completed 12 weeks of transdermal nicotine week open-label outpatient study. Patients were non-smoking, and depression was defined as being ≥15 on the Montgomery-Asberg Depression Rating scale (MADRS). Transdermal nicotine patches were applied daily and titrated to a maximum dose of 21.0 mg/day, however we also allowed dose reductions for tolerability. The EEG sessions were completed at baseline and following nicotine treatment, in which patients completed an auditory oddball and cued go-nogo tasks. Results showed a significant decrease in depressed mood as measured by the MADRS across the 12 weeks (μ=17, p<0.01). Behaviorally, patients improved in speed from baseline to post-treatment; however there were no strong electrophysiological differences on treatment alone. Examining the change in mood however, showed that patients with greater improvement in depressed mood showed improved electrophysiological performance. This preliminary data indicates that transdermal nicotine may be a promising therapy for patients with LLD. However, without a placebo-controlled group we cannot confirm the benefits on mood and electrophysiology.